Volume 5
Number 3
March 2026
Pages 609–918

Environmental Science Advances

rsc.li/esadvances

ISSN 2754-7000

ROYAL SOCIETY OF CHEMISTRY

PAPER

Norman Kelly, Peter Boelens, Jens Gutzmer *et al.*
Hydrometallurgical recovery of high-purity copper from waste printed circuit boards: an experimental study and life cycle assessment

Environmental Science Advances

ROYAL SOCIETY OF CHEMISTRY

PAPER

View Article Online
View Journal | View Issue

Cite this: *Environ. Sci.: Adv.*, 2026, **5**, 772

Hydrometallurgical recovery of high-purity copper from waste printed circuit boards: an experimental study and life cycle assessment

Norman Kelly, †*[a] Peter Boelens, †*[ab] Ashak Mamhud Parvez, [ac] Sabine Kutschke, [a] Doreen Ebert, [a] Bradley Martin Guy, [a] Robert Möckel, [a] Muhammed Haseeb Aamir,[a] Cynthia Sanchez-Garrido, [a] Ulrike Fischer,[a] Mohsin Sajjad, [a] Axel D. Renno, [a] Lucas Ott, [d] Frank Ellinger, [d] Ajay Bhagwan Patil [ae] and Jens Gutzmer *[a]

Due to their complex structure and high metal content, printed circuit boards (PCBs) represent both a major challenge and opportunity for recycling. By weight, copper represents the main metallic fraction of PCBs. Thus, the selective removal and recovery of high-purity copper is crucial for efficient recycling, in addition to the extraction of minor, precious metal components, such as gold, silver, and palladium. This paper presents an integrated study of detailed characterization, process development, and the environmental impact of copper recycling from virgin PCBs using hydrometallurgical approaches – rather than the well-established pyrometallurgical route. Thorough mineral liberation analysis helped us understand specific processing and metallurgical approaches based on the accessibility of the target metal phases. Near quantitative copper leaching was achieved with H_2SO_4/H_2O_2 and HNO_3, whereas heterotrophic bioleaching with citric acid and polyglutamic acid resulted in <13% of copper leaching. In a two-stage process, >98% of the leached copper was selectively transferred to the organic phase by solvent extraction with a LIX 84-I-kerosene/$CuSO_4$–H_2SO_4 system. With the exception of Ni^{2+}, co-extraction of further metal ions was not detected. Subsequently, up to 98% of the copper was recovered from the organic phase *via* stripping with a model electrolyte containing copper(II) sulfate in H_2SO_4. From the enriched electrolyte solutions, metallic copper with a purity of 99.64–99.84% was electrodeposited on a stainless steel cathode, with a current efficiency of 98.66–99.85%. Residual copper obtained by washing the leaching residue was recovered by cementation with an iron powder according to a stoichiometric ratio of Fe/Cu^{2+} of 1.5 : 1. According to life cycle assessment, based on the energy and chemical consumption of the copper recycling process, the global warming potential of the tested approaches lies in the range 13.0 kg CO_2 eq. per (kg Cu) – 40.3 kg CO_2 eq. per (kg Cu). The greatest contributors to environmental impact are leaching and solvent extraction processes, which can be substantially improved by operating on a larger scale and recycling process ingredients. The proposed approach demonstrates end-to-end high-purity metal recovery with direct application to various circuit boards and copper-rich electronic components.

Received 7th October 2025
Accepted 14th January 2026

DOI: 10.1039/d5va00348b

rsc.li/esadvances

Environmental significance

The rapidly growing stream of waste electrical and electronic equipment (WEEE) presents major environmental challenges, with printed circuit boards (PCBs) being particularly critical due to their high metal content and complex structure. This study presents a novel hydrometallurgical process for the selective recovery of high-purity copper from PCBs, supporting circular economy strategies. Combining leaching, solvent extraction, stripping, and electrowinning, the process achieves copper recoveries of up to 98% and purities of 99.64–99.84%. Life cycle assessment shows a global warming potential comparable to pyrometallurgical routes. Lower capital demand, scalability, and suitability for decentralized operation highlight the environmental potential of this hydrometallurgical approach for more sustainable WEEE recycling.

[a]*Helmholtz-Zentrum Dresden-Rossendorf, Helmholtz Institute Freiberg for Resource Technology, Freiberg, Germany. E-mail: p.boelens@hzdr.de; n.kelly@hzdr.de; j.gutzmer@hzdr.de; Tel: +493512604400*

[b]*TU Dresden University of Technology, Institute of Semiconductors and Microsystems, Dresden, Germany*

[c]*TU Dresden University of Technology, Institute of Waste Management and Circular Economy, Pirna, Germany*

[d]*TU Dresden University of Technology, Chair for Circuit Design and Network Theory, Dresden, Germany*

[e]*University of Jyväskylä, Faculty of Mathematics and Science, Department of Chemistry, P.O. Box 35, Jyvaskyla, FI-40014, Finland*

† Authors with the equal contributions.

1. Introduction

Waste electrical and electronic equipment (WEEE) is one of the fastest-growing solid waste streams globally. In 2022, 62 Mt of WEEE were produced globally, containing metals valued at an estimated 91 billion USD. With an estimated value of 19 billion USD, copper is one of the most valuable metal components in WEEE.[1] Printed circuit boards (PCBs) are characterized by a particularly high metal/copper content[2] and an exceptionally complex structure. They also represent a considerable fraction of WEEE (3–8%) by weight in large and small appliances respectively.[3] A comparison of different types of WEEE has been reported in the literature, suggesting that the smallest fractions of PCBs occur in refrigerators (0.5% weight) and the largest in cell phones (37.6%).[4] The same authors also noted considerable differences in the metal content of PCBs according to the type of WEEE considered (see Table 1).

Selective recovery of copper, the major metallic component of waste PCBs by weight, is thus a crucial aspect of existing PCB recycling schemes.[5] Selective removal of copper from PCBs not only allows for the recycling of the main metallic component but also enhances the recyclability of minor components, such as precious metals (*e.g.*, gold, silver, and palladium; see Table 1).

Furthermore, for the first time in 2023, the European Union acknowledged copper as a strategic raw material due to its indispensability for the energy transition.[6] Numerous studies have investigated metallurgical recoveries of waste PCBs,[7–9] but have usually focused on individual process steps, such as comminution, leaching, or extraction, without a systematic end-to-end approach to high-purity copper recovery. Very few studies compare the environmental impacts of the process routes required for high-purity copper recycling from PCBs. Yet, this systemic perspective is crucial for assessing the economic and environmental impacts associated with novel process schemes at an early stage of development. From Table 1, it is evident that a high proportion of PCB content in e-waste correlates with a high copper and precious metal content. Such high-value e-waste increases the viability of recycling and the circular economy approach.[10] Furthermore, by enriching metallic fractions through physical separation prior to hydrometallurgical treatment, pre-concentration enhances process efficiency and thereby increases the overall economic viability of PCB recycling.[11]

Life cycle assessment (LCA) is a well-established approach to evaluate the potential environmental impacts of a product throughout its life cycle from raw material acquisition, through production, use, end-of-life treatment, recycling, and final disposal. Through this systematic perspective, the shifting of potential environmental and cost burdens between life-cycle stages or individual processes can be identified and possibly avoided.[12] LCA of copper production has been extensively studied, and results vary with ore grade, production technology, energy systems, assessment boundary conditions, and calculation methods.[13] Previous studies have mainly focused on the beneficiation of copper ore[14] and pyrometallurgical refining as accepted industrial practice of primary[15–20] and secondary copper production.[15–17,21,22] In contrast, very few LCA studies have been conducted on copper production through a hydrometallurgical route.[16,23,24]

As the energy costs for pyrometallurgical processes are mounting, and due to the complexity of e-wastes in composition, hydrometallurgical processes are becoming increasingly relevant. Scalable, end-to-end processes must be developed through viable process sheets, with a clear understanding of their impact. This manuscript uses simple chemical processes to demonstrate the valorization of complex PCB e-waste into pure metal products, along with a detailed life-cycle assessment of the processes used. By taking such a holistic approach, the contribution adds a technologically sound perspective on the practical application of hydrometallurgical processes for the recovery of metals from waste electronics.

In the present study, we present a thorough characterization and liberation analysis of PCBs to understand suitable process targets, as well as an end-to-end process detailing the recovery of high-purity copper by testing different leaching approaches on waste PCB feeds (chemical and bio-based), followed by selective solvent extraction (SX), stripping, and electrowinning (EW). For this purpose, we have generated systematic experimental data at the laboratory scale, enabling us to perform LCA for an integrated processing scheme to recycle copper from PCBs and produce pure copper. Finally, we compare the LCA results of our developed process with those of more established approaches for the recovery of copper from primary and secondary sources. The process resulted in high copper recovery and purity, with an impact comparable to that of established pyrometallurgical methods.

2. Materials and methods

The materials used for this study include PCBs and various reagents, while the methods are categorized into comminution,

Table 1 Weight fraction of PCBs, plastic and ferrous material in selected WEEE types modified after[4] along with corresponding contents of copper, gold, silver and palladium in PCBs. BDL: below detection limit

	Weight fraction in WEEE			Weight fraction in PCB			
WEEE type	PCB (%)	Plastic (%)	Ferrous (%)	Cu (%)	Au (ppm)	Ag (ppm)	Pd (ppm)
Refrigerator	0.5	43.7	47.6	17	44	42	BDL
Washing machine	1.7	35.3	51.7	7	17	51	BDL
LCD TV	11.6	31.8	43	18	200	600	BDL
Laptop	13.7	25.8	19.5	19	630	1100	200
Cellular phone	37.6	37.6	0.8	33	1500	3800	300

analytical methods, bioleaching, chemical leaching, SX, EW, washing and cementation, and LCA.

2.1. Printed circuit boards

Commercially available unpopulated/virgin PCBs were used for our experiments. Since electrical components were not attached to the PCBs, the characterization and quantification of the "pure PCB" were possible.

2.2. Comminution

Size reduction of the PCBs was first performed using a Pulverisette 19 type cutting mill (Fritsch GmbH, Idar-Oberstein, Germany). The obtained material was subsequently milled with a 6875D type cryomill (SPEX SamplePrep, New Jersey, USA) using about 0.13 L min^{-1} liquid nitrogen (Linde GmbH, Pullach, Germany). Finally, about 160 g of fine-grained material (d_{50} $\approx$ 125 μm) was obtained. For analytical characterization and leaching experiments, this material was sub-sampled using a rotary sample splitter.

2.3. Bioleaching

It is known that heavy metals in PCBs inhibit microbial growth and metabolism; therefore, bioleaching experiments were performed using spent medium as in Beiki *et al.* (2023).[38] For bioleaching experiments, supernatant solutions of heterotrophic microbial cultures were used. A culture broth rich in polyglutamic acid was produced with *Bacillus licheniformis* DSM8785 according to a procedure reported elsewhere[25] without glutamic acid and centrifuged with a LYNX6000 (Thermo Fisher Scientific) at 10 000 g (centrifugal force) for 10 minutes. Concentrated citric acid was obtained through the cultivation of *Yarrowia lipolytica* DSM3286 as reported in Papanikolaou *et al.* (2002).[26] The biomass of this culture was removed by centrifugation at 10 000*g* for 10 minutes with a CARR9010 Powerfuge Pilot (CARR Biosystems). The supernatant of DSM8785 with polyglutamic acid was diluted to a concentration of 30 g L^{-1} at pH 4.8, and the supernatant of DSM3286 with citric acid was diluted to 30 g L^{-1} at pH 5.4. In 15 mL tubes, 0.6 g of cryo-milled PCB was suspended with 6 mL of one of the leaching media, resulting in a pulp density of 10%. The samples were incubated in an overhead shaker at room temperature (r.t., *i.e.* 20–25 °C). The tubes were removed from the overhead shaker after 2, 12, 24 and 48 hours of incubation and centrifuged at 3450 rpm for 10 min. Finally, the dissolved concentrations of copper, gold and nickel in supernatant were analyzed in iCAP RQ (Thermo Fisher Scientific) ICP-MS. The effect of factors such as leaching time and selection of spent medium for bioleaching has been optimized.

2.4. Chemical leaching

The effects of factors such as acid concentration, feed particle size, oxidant concentration (H_2O_2), solid-to-liquid ratio, and direct *vs.* stepwise addition of oxidant were tested and optimized step by step. The experiments were performed in duplicate, and resulting mean values and half ranges ($n = 2$) are shown in the plots.

Small-batch leaching experiments with 250 mg of cryo-milled PCB material were carried out in duplicate in 6 mL glass vials on a multi-stirrer (VELP Scientifica). Defined volumes of 5 M H_2SO_4, 5 M HNO_3, 30 wt% H_2O_2 solution, and water were added to the material, and the reaction mixture was stirred at room temperature (r.t.) In the case of a strong reaction, H_2O_2 was added over an extended period of 5 min. After completion of the reaction time, the reaction mixture was transferred to a tube and centrifuged at 15 557 g. The solution was decanted, and the residue was washed 3 times with 3 mL of water, then dried for 48 h at 55 °C.

After the small-scale investigations, suitable experimental parameters were selected for both leaching systems. Single experiments were carried out, each with scaled conditions using 11.5 g of the feed material (*i.e.*, comminuted PCBs). In the case of the leaching medium with H_2SO_4/H_2O_2, a concentration of 3 M for H_2SO_4 and 3 wt% H_2O_2 at S/L of 1 : 10 and a reaction time of 4 h were selected. H_2O_2 was added over a period of 1 h. In contrast, a concentration of 3 M and a solid-to-liquid ratio (S/L) of 1 : 3 was used for HNO_3. The reaction time was 2.5 h and showed an increased formation of nitrous gases at the beginning. The reaction mixtures were then transferred to 50 mL tubes and centrifuged two times (each 1 × 2 min, 1 × 9 min at 15 557 g). The leaching solution was separated by pipetting, and the residue was used for further washing treatment.

2.5. Solvent extraction

Solvent extraction experiments were conducted at r.t. in 800 mL beakers. In the extraction step, defined volumes of the corresponding leachate and the organic phase were added to the beaker. Mixing of both phases was conducted with an RW 20 overhead stirrer (IKA). After a defined mixing duration, a 5804 G type centrifuge (Eppendorf) was used to ensure complete phase separation. Samples of the aqueous and/or organic phase were collected for analysis. A pH electrode (Mettler Toledo InLab Micro, Ag/AgCl, 3 M KCl) was used to measure the pH in the preferred pH range of 1.2–1.8. The pH was adjusted by the addition of 10 M NaOH solution. Depending on the type of leachate, two or three extraction steps were carried out in sulfuric acid and nitric acid media, respectively.

All organic phases were combined after the extraction step was complete. For the following stripping process, a solution of copper(II) sulfate ($c(Cu^{2+})$ = 34.3 g L^{-1} in 2 M H_2SO_4) as a synthetic electrolyte was brought into contact with the corresponding loaded organic phase. The re-extraction procedure was comparable to the extraction steps described above. The element concentrations in aqueous phases were analyzed by ICP-OES. The presence of residual copper(II), as well as the conditioning of the organic phase after the SX experiments, was monitored with FT-IR spectroscopy.

2.6. Electrowinning

For the EW experiments, an electrolytic cell was placed over the magnetic stirrer, and the electrodes (1 cathode: SS 1.4301; 1

anode: Pb) were connected to a suitable power source (Joy-IT PS1440-C). The stirring bar was placed between the electrodes at equal distances. Thereafter, the prepared solutions of 400 mL per experiment were poured into the electrolytic cell. The solutions contained 50% of the stripped copper solution and 50% of a copper(II) sulfate solution (34.3 g L^{-1} Cu^{2+} in water) in order to provide sufficient volumes for the experiment. For the solutions based on the chemical leaching and SX experiments, a current density of 30 mA cm^{-1} and a current of 0.60 A were selected. The temperature range of the experiment was maintained between 20–23 °C. The samples of the electrolyte ($V = 5$ mL) were obtained at the start of the experiment and during the experiment (after 5 min, 15 min, 30 min, 45 min, 1 h, 2 h, 3 h, and 4 h). The voltage and current were monitored every hour from the power source display and validated with an additional voltmeter. After the experiment, the deposited metallic copper was removed from the cathode and characterized with the S1 TITAN handheld XRF analyzer by using the Alloy2 application supplied by Bruker. Element concentrations in aqueous phases were analyzed by ICP-OES; TOC before and after the experiment was determined with a Sievers InnovOx ES Laboratory TOC Analyzer Veolia). Deposited Cu pieces were examined for cross-section structure and composition by a scanning electron microscope with an energy dispersive X-ray detector. Different phases were explored to assess the quality/purity of deposition.

2.7. Washing and cementation

The two residues from larger batch-scale experiments (H_2SO_4/H_2O_2 and HNO_3) were washed once with 18 mL and five times with 20 mL of distilled water. The material was initially suspended in water in a 50 mL Eppendorf tube, and mixing continued on an overhead shaker (Heidolph Reax 2) for 15 minutes. After centrifugation, the aqueous phase was decanted, and the washed residues were dried at 55 °C in an oven (Memmert UF 260). Metal concentrations in the wash water were determined with ICP-OES as described in the section above.

Selected samples from washing procedures were further treated in cementation experiments. First, 10 mL of the wash water was placed in a 20 mL beaker with a magnetic stirring bar on a multi-position magnetic stirrer (VELP Scientifica). Iron powder was added to the solution according to the stoichiometric ratio $Fe/Cu^{2+} = 1.5:1$. The mixture was stirred for 1 h at r.t. Once the reaction was complete, the aqueous solutions were removed after centrifugation and decantation. The brownish cementate was washed three times with water and dried at 55 °C. The cemented sample materials were characterized with the S1 TITAN handheld pXRF analyzer by using the GeoChem application supplied by Bruker.

2.8. Analytical methods

A number of analytical techniques were utilized for the characterization of comminuted PCBs. These include phase identification and quantification by X-ray characterization techniques and elemental measurements, which determined the concentrations of dissolved ions, carbon, hydrogen, nitrogen, and sulfur in solid PCBs (with and without hydrometallurgical treatment). Finally, vibrational spectroscopy was also carried out to investigate the interaction between copper and the extractant in the organic phase.

2.8.1. Mineral liberation analysis. A Thermo Fisher Scientific (FEI) Mineral Liberation Analyzer (MLA) 650F, equipped with two XFlash Bruker detectors (5030), was used for automated mineralogical analysis. Automated mineralogy combines backscattered electron (BSE) grey-scale intensities with energy dispersive spectroscopy (EDS) to segment, identify, and quantify solid phases. Bruker Esprit software was used to collect and quantify X-ray spectra, and MLA Suite was used for measurement acquisition (v. 3.1.4.686), data processing, and reporting (v. 3.1.5.993). Sample preparation included the mounting of cryo-milled PCB material into a single 30 mm epoxy grain mount. Prior to MLA analysis, this grain mount was polished, cleaned with ethanol, and carbon-coated using a Leica MED 020 vacuum evaporator. The operating conditions of the Scanning Electron Microscopy (SEM) were an accelerating voltage of 25 kV, spot size of 5.7, specimen current of 10 nA, and a working distance of 13 mm. The GXMAP measurement mode was used, with a horizontal field width of 1000 microns, a dwell time of 16, a pixel resolution of 1000, and an X-ray step size of 4 microns.

2.8.2. X-ray powder diffraction. X-ray powder diffraction (XRD) was used to characterize the phase composition of cryo-milled feed material, as well as residues from leaching and bioleaching experiments. A PANalytical Empyrean device, equipped with a PIXcel 3D medipix detector, a Co-tube (Fe-filter), and an automated divergence slit (to keep the irradiated area constant), was used for the analyses. Depending on the amount of available sample material, the powders were either filled into 16 mm sample holders (diameter) or placed in low-background silicon sample holders. The initial sample material was filled in 27 mm sample holders. Phase identification was performed using the pdf-5+ 2024 database (provided by ICSD).

2.8.3. X-ray fluorescence spectroscopy. A PANalytical Axios Max (Malvern Panalytical) wavelength-dispersive X-ray fluorescence (WDXRF) device was used for whole-sample chemical characterisation. Initially, 10 g of cryo-milled sample material was thoroughly mixed with 2 g wax (Cereox©) to produce a 40 mm pressed pellet. Data evaluation was performed using the fundamental parameter-based OMNIAN programme provided by PANalytical. For material amounts less than 10 g resulting from leaching experiments, chemical analyses were performed with an S1 TITAN energy-dispersive handheld XRF analyzer using the two commercial applications Alloy2 and GeoChem (Bruker). Sample preparation was not required. While the Alloy2 application is calibrated for materials with a metal or alloy matrix, the GeoChem application is calibrated for an oxidic sample matrix. The device is equipped with the Rh tube. The measurement time was 1 min per sample.

2.8.4. Inductively coupled plasma atomic emission spectroscopy and inductively coupled plasma mass spectrometry analysis. Inductively coupled plasma optical emission spectrometry (ICP-OES) and mass spectrometry (ICP-MS) were used for the determination of selected trace element contents (*e.g.*, Au) of the cryo-milled feed samples, as well as the chemical

analysis of leach solutions. For these measurements, the sample was completely digested using two different approaches in an Anton Paar microwave digester, Multiwave 5000, with the 20SVT50 rotor. For the first digestion approach, 0.2 g sample material was dissolved with aqua regia (3 : 1 ratio of HCl 30% and HNO_3 67–69%) and for the second approach, 0.1 g sample material was digested in HF (48%) and HNO_3 (67–69%) in a ratio 1 : 3. Sample/acid mixtures were heated to 230 °C for 30 min in the microwave. After the HF digestion, the sample solution was complexed with 12 mL saturated H_3BO_3 to neutralize excessive HF. While aqua regia digestion reliably dissolved all metallic components, HF digestion ensured complete digestion, including all organic and silicate components. The solutions were diluted and subsequently analyzed using a Plasmaquant PQ 9000 ICP-OES (Analytik Jena) and Nexion 300X ICP-MS (PerkinElmer) for their elemental content.

2.8.5. CHNS and total organic carbon analysis. A Vario EL cube (Elementar Analysen System GmbH) was used for carbon, hydrogen, nitrogen, and sulfur determination. The device employs argon as carrier gas with a pressure of 1200–1250 mbar and a flow rate of 230 mL min^{-1}. Oxygen was used for washing the tubes (at 10 mL min^{-1}) and for combustion (combustion time of 80 s at 35–40 mL min^{-1}). The samples from the cryomill, the bioleaching, and the leaching residues were analyzed with fivefold repetitions. The mass of each individual sample varied between 5.0 and 6.6 mg. A correction factor was applied to the concentrations of carbon, hydrogen, nitrogen, and sulfur, based on the analysis of a 5 mg sulfanilamide reference.

In addition, total organic carbon (TOC) concentrations in raffinates and model solutions from selected processes were determined with a Sievers InnovOx ES Laboratory TOC Analyzer (Veolia) based on a supercritical water oxidation process.

2.8.6. Fourier-transform infrared spectroscopy. A Cary 630 spectrometer (Agilent) was used for the measurement of Fourier-transform infrared spectroscopy (FT-IR) of selected organic phases. The sample carrier was loaded with 20 µL analyte, and the absorption spectra were detected with a DialPath unit at a distance of 30 microns. Measurements were carried out at a temperature of 20 ± 2 °C with 32 scans per sample. Background scans were done (32 in total), using a wavenumber range from 650 to 4000 cm^{-1} and with a resolution of 2 cm^{-1}. Data were processed and extracted using MicroLab Software.

2.9. Life cycle assessment

To conduct LCA, the ISO standard 14 040 (ref. 12) was followed. The LCA consists of four steps: (1) goal and scope definition; (2) life cycle inventory (LCI) analysis; (3) life cycle impact assessment (LCIA), and (4) interpretation. The system boundary for these processes begins with the delivery of end-of-life waste PCBs (WPCBs) to the treatment facility. It ends with the electrodeposition of metallic copper with a purity of 99.6–99.8% that are qualified to re-enter the market (gate-to-gate approach), as shown in Fig. 1. Any emissions generated and the treatment of all wastes produced during the processing of copper were included in the LCA. To assess the impact of copper recovery, the functional unit was 1 kg of copper.

The Life Cycle Inventory (LCI) was established using the Ecoinvent 3.8 database. For the purpose of this study, reagents, energy, emissions, and waste were categorized as technospheric and elementary flows, while the feed materials were regarded as intermediate flows, and electrowinned copper was defined as the product flow. This process involves compiling and quantifying input and output data within the defined system boundary, accounting for the movement of materials, energy, waste, and resources,[27] as shown in Fig. 1. Table S1 in the SI lists all energy and resource providers used in the overall production process in Ecoinvent to link the LCI in OpenLCA.

The Life Cycle Impact Assessment (LCIA) entails categorizing inventory data and linking these to distinct environmental impact categories.[28] Typical impact categories consist of 18 midpoint impact categories, such as global warming potential

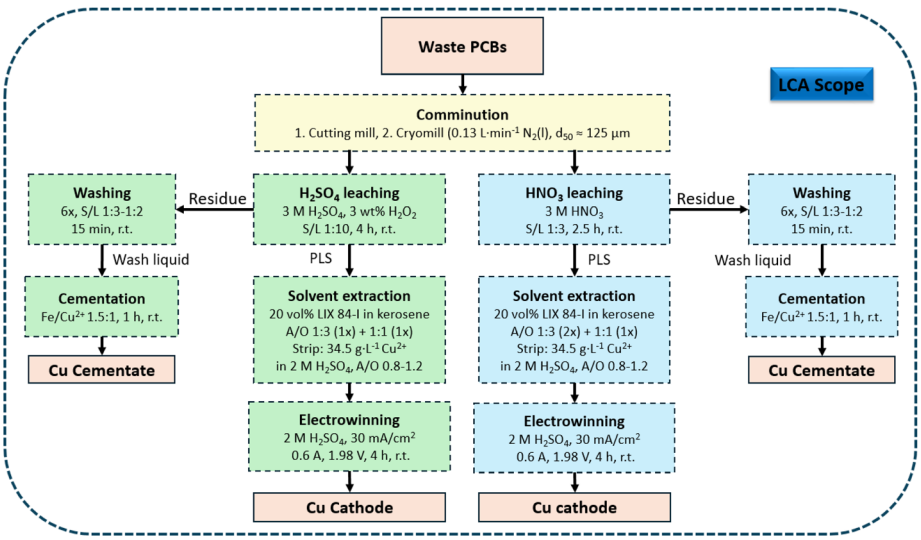

Fig. 1 Detailed process flow sheet and LCA boundary conditions in the present work.

Table 2 Selected inventory results, inputs, and outputs per kilogram of copper. '—' means this entry is not part of the respective unit process

Inputs	Unit	Comminution	H_2SO_4	HNO_3
Printed circuit boards waste	g	4096.90	—	—
Electricity, medium voltage	kWh	1250.45	427.59	427.59
Nitrogen	kg	103.31	—	—
Hydrogen peroxide, without water, in a 50% solution state	g	—	5899.54	—
Sulfuric acid	g	—	43 452.08	31 011.76
Water, decarbonised	g	—	2 78 892.06	1 88 888.49
Iron pellet	kg	—	43 961.52	89 601.00
Sodium hydroxide, without water, in a 50% solution state	g	—	8407.55	641.25
Benzaldehyde, 2-hydroxy-, oxime	g	—	25 450.66	9846.81
Nitric acid, without water, in a 50% solution state	g	—	—	3883.15
Outputs				
Leaching residue	g	—	3437.12	2715.00
Waste water	g	—	21 375.13	21 018.88
Chemical, organic	g	—	1 30 032.06	50 587.82
Copper sulfate	g	—	3 39 864.62	2 66 761.67
Copper, cathode	g	—	1000.00	1000.00
Depleted electrolyte	ml	—	1 42 500.89	1 42 500.89
Gold, unrefined	g	—	9.83×10^{-1}	9.83×10^{-1}
Iron, unrefined	g	—	1.10×10^{0}	9.69×10^{-1}
Nickel, unrefined	g	—	7.34×10^{0}	4.85×10^{0}

(GWP100) and terrestrial acidification potential (TAP100) over 100 years, eutrophication, ozone depletion, and others. The ReCiPe 2016 (H) method was used due to its extensive use as an LCIA method. For proper interpretation, the results of both LCI and LCIA are summarized and deliberated, considering the defined goal, scope, limitations, and sensitivity analysis within the secondary copper production process (Table 2).

3. Results and discussion

The following section presents the experimental and sustainability results of hydrometallurgical Cu recovery from printed circuit boards, beginning with material characterization and proceeding through bioleaching, chemical leaching, SX, EW, washing, and cementation, before concluding with a life cycle assessment.

3.1. Characterization

Phase characterization by XRD and MLA provided insights into the composition of the PCBs and their amenability to hydrometallurgical treatment. Similarly, elemental analyses (*i.e.*, XRF, ICP-OES, and ICP-MS) helped to track the performance of the hydrometallurgical experiments. The major elemental composition of the milled PCBs (see Table 3) is in good agreement with PCB compositions reported elsewhere.[4]

As confirmed by XRD and MLA data, barium is present in the form of barite ($BaSO_4$), a typical filler material in the solder mask, and as a trace constituent of some of the glass phases.

Table 3 Elemental composition of the PCBs

Method	Element	wt%
XRF	Cu	12
XRF	Si	18.7
XRF	Ca	12.1
XRF	Ba	1.2
XRF	Al	5.8
XRF	Ni	0.2
XRF	S	0.4
XRF	Br	7.5
CHNS	C	20.7
ICP-MS	Au	0.05

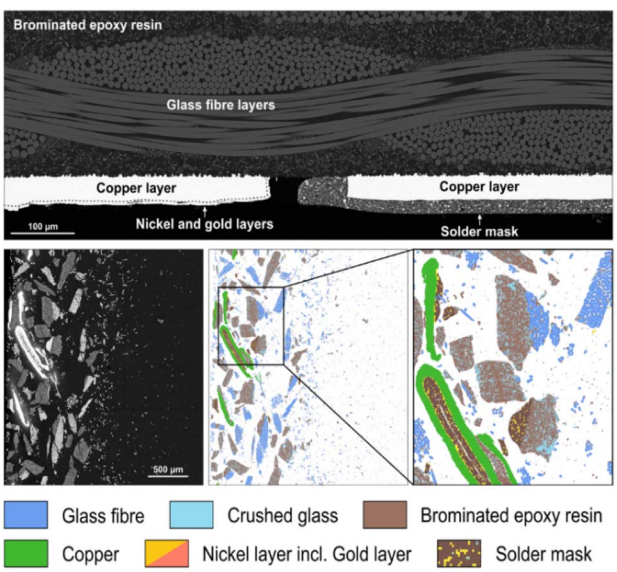

Fig. 2 BSE image of a PCB's cross section (upper part) with the typical structure of composite material composed of glass particles covered by brominated epoxy resin and glass fibre layer of the substrate plate, copper layer, solder mask. including *e.g.* barite particles and other fillers and Ni–Au layers covering exposed copper layers. The lower part depicts the same material crushed: BSE image (left) and MLA false colour image (right).

Other inorganic fillers in the solder mask include glass particles and talc, as derived from MLA data. Silicon, calcium, and aluminum are mainly derived from the glass fibre in the substrate plates, as well as in glass particles in the organic parts of the plate (see Fig. 2). Organic carbon is derived from both the substrate plate and solder mask, while bromine is present in the flame retardant in the base plate. Sulfur is mainly bound to barite. Though sulfur and barium contents are consistent, CHNS analysis yielded significantly lower sulfur values, likely due to the high decomposition temperature of barite.[29] The metallic components, such as copper, nickel and gold, are invariably part of the electric conductive tracks of the PCBs. The characterized morphology for the virgin PCBs can be a good starting point to understand, from a process point of view, in comparison to more complex e-wastes with attached components.

A cross-section of one of the PCBs that were used for recycling experiments is depicted in Fig. 2. It shows the architecture commonly encountered in modern PCBs. SEM-BSE and MLA images (Fig. 2) reveal that there is a central substrate of glass fibre and brominated epoxy resin. On this base, the conductive tracks of copper, nickel and gold are situated, which are surrounded by the solder mask comprising epoxy resin with different fillers. Fig. 2 also illustrates that the metal layers, albeit very thin, can be accessible to the hydrometallurgical leaching even without the need for comminution. The quantitative phase composition of the crushed PCBs is presented in Table 4. Both the BSE and false colour image from MLA illustrate the comminution results of the PCBs by means of particle shape, size and liberation.

3.2. Bioleaching

In the bioleaching experiments, with polyglutamic acid (pH 4.8) and citric acid (pH 5.4), the concentrations of leached Cu^{2+}, Au^{3+}, and Ni^{2+} ions were analyzed over time (see Fig. 3). Modest leaching performances were observed for all three metals, with the highest value being approximately 20% for Ni in polyglutamic acid. Copper leaching remained below 13% using these two lexiviants. In both experiments, the dissolved metal concentrations stagnated after 48 h, indicating that recovery was not considerably limited by the contact time with the leaching media. After 48 h, the concentrations were in the range of $c(Cu^{2+}) = 1000–1400$ mg L^{-1}, $c(Au^{3+}) = 0.8–1.2$ mg L^{-1}. and $c(Ni^{2+}) = 35–60$ mg L^{-1}. Polyglutamic acid was the most effective leaching medium for copper and nickel, while the highest amount of gold was leached in citric acid.

Table 4 Quantitative phase composition of the crushed material as derived from MLA analysis

Compound	wt%
Brominated epoxy resin	28.6
Glass fibre	41.8
Crushed glass	13.6
Barite	1.0
Metallic copper	14.6
Metallic nickel	0.3
Metallic gold	0.02

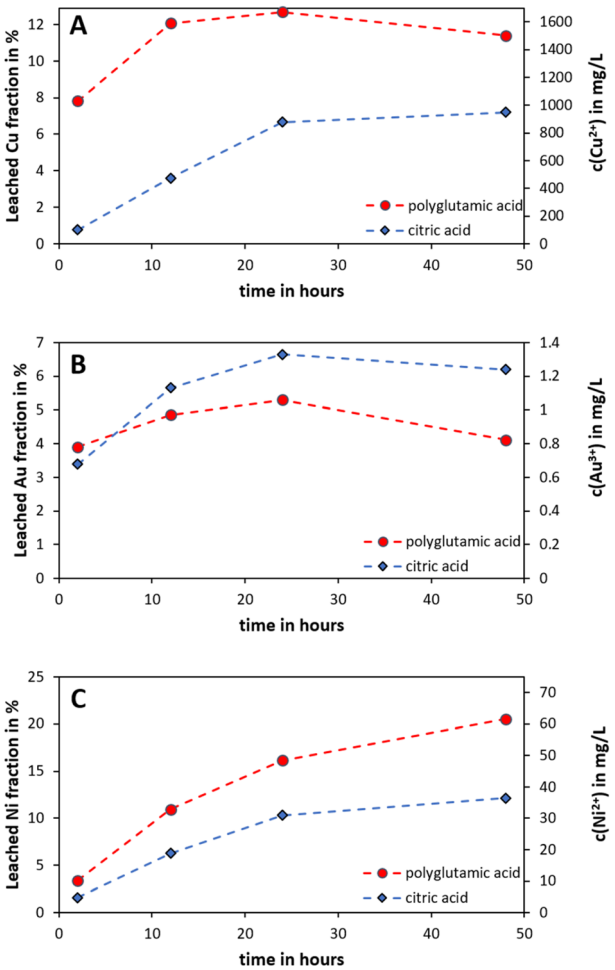

Fig. 3 Evolution of the fractions and concentrations of (A) Cu^{2+}, (B) Au^{3+} and (C) Ni^{2+} leached in polyglutamic acid and citric acid.

Chemolithotrophic acidophilic bacteria are known to leach metals such as copper, zinc, gold, and silver from printed circuit boards (PCBs) through acidolysis and redoxolysis. Copper recovery can reach 93% to 100%,[30,31] zinc recovery up to 70%,[31] and gold recovery up to 44%.[32] Fungi and Streptomyces represent another major group of microorganisms capable of leaching metals from PCBs through acidolysis and complexolysis. Studies have demonstrated that fungi and Streptomyces can leach 82% to 100% zinc, 80.39% to 81% nickel, 68% to 85.88% copper,[33,34] 44% to 56% silver,[34,35] and 0.5% to 42.5% gold.[35,36] Additionally, cyanide-producing bacteria have been used for leaching precious and valuable metals from PCBs by forming stable metal-cyanide complexes. These bacteria have been shown to recover 10.8% to 69% gold, 36.2% to 90% silver, and 11.4% to 79% copper.[37–41]

Overall, comparability among these studies remains limited due to variations in leaching time, the choice of 1-step, 2-step, or spent-medium approaches, and the use of supplementary redox components like H_2O_2. The different bioleaching approaches lead to varying degrees of metal mobilization,

influenced by factors such as the PCB composition, leaching duration, and pulp density. In the present study, using spent medium from a Yarrowia lipolytica culture over a period of two days, leaching yields of 6% copper, 6.5% gold, and 10% nickel were achieved. These results are comparable to those reported by Faraji *et al.* (2018). Additionally, using spent medium from an Aspergillus niger culture, a 10% PCB suspension was leached.[33] The spent medium contained citric acid, oxalic acid, and other organic acids as lixiviants, resulting in the solubilization of 7.4% copper, 85.5% zinc, and 44.9% nickel within 21 days.

3.3. Chemical leaching

3.3.1. Batch scale leaching experiments. For the extraction of copper, nickel, and gold, as well as a possible contamination of iron from the ground PCB samples, leaching tests were initially carried out with H_2SO_4/H_2O_2 and HNO_3/H_2O_2 while varying the concentrations of H_2O_2 (0–9 wt%) at r.t. (see Fig. 4A). As expected, blank tests with water showed that none of the metals dissolved under the selected conditions. In the case of H_2SO_4 (3 M) and H_2O_2 as a leaching medium, there was a significant increase in the copper concentration up to 3 wt% of H_2O_2. This can be attributed to the low oxidizing power of H_2SO_4 at this concentration and the selected conditions. In the case of HNO_3, a high copper extraction with 15 600 ± 900 mg L^{-1} was achieved even in the absence of H_2O_2. Accordingly, H_2O_2 was not used for further experiments with HNO_3. Comparable trends were also observed for nickel leaching performance. In the case of H_2SO_4/H_2O_2, the nickel concentrations were 104–252 mg L^{-1}, while for HNO_3/H_2O_2 they were 182–242 mg L^{-1}. The concentration of iron in solution remained largely unaffected by the choice of parameters and was between 30–40 mg L^{-1}. The small amount of iron is attributed to contamination during comminution of the PCBs by the steel milling equipment.

Leaching by H_2SO_4/H_2O_2 (3 wt%) and HNO_3 was considered for further investigation. The concentration of the acids used was varied (Fig. 4B). A strong increase in copper leaching was observed for both leaching systems up to an acid concentration of 1 M. Below this concentration, H_2SO_4/H_2O_2 shows a significantly higher extraction than HNO_3. This is due to the fact that the oxidizing agent H_2O_2 is already present in the reaction mixture, and the leaching yields are largely dependent on the stoichiometric amount of acid required for dissolution. In the case of HNO_3, oxidation of the metallic copper can only be expected at higher acid concentrations, resulting in lower leaching yields at acid concentrations of 0.1–0.5 M. At concentrations of 1–3 M, the yields become increasingly similar to those of the H_2SO_4/H_2O_2 system. The extraction of nickel in the H_2SO_4/H_2O_2 leaching system is largely independent of acid concentrations between 0.25 M to 3 M resulting in nickel concentrations of 220–290 mg L^{-1}. In contrast, the nickel concentrations are significantly lower when HNO_3 is used; they are only 198–240 mg L^{-1} at acid concentrations of 1–3 M. The extraction of iron is not particularly affected by the acid concentration, and is comparatively lower for HNO_3 (10–20 mg L^{-1}) than for H_2SO_4/H_2O_2 (30–60 mg L^{-1}). For both leaching systems, a continuous increase was observed up to a total reaction time of 2 hours (Fig. 6).

$$Cu(0)_{(PCB)} + H_2O_2 + H_2SO_4 \rightarrow Cu(II)SO_{4(aq)} + 2H_2O \quad (1)$$

Copper in its metallic state is present in the solid phase (*i.e.*, with PCB feeds). The oxidation of this metallic Cu(0) to the soluble state in the sulfate medium, Cu(II) sulfate, required oxidative pathways of leaching. To enable such a reaction, only sulphuric acid is not sufficient, as evident from the reaction kinetics. Here, hydrogen peroxides, with the ability to provide an *in situ* oxidative environment *via* the release of oxygen, help accelerate leaching by converting Cu(0) to the Cu(II) state, which then forms sulfate in solution, as shown in eqn (1).

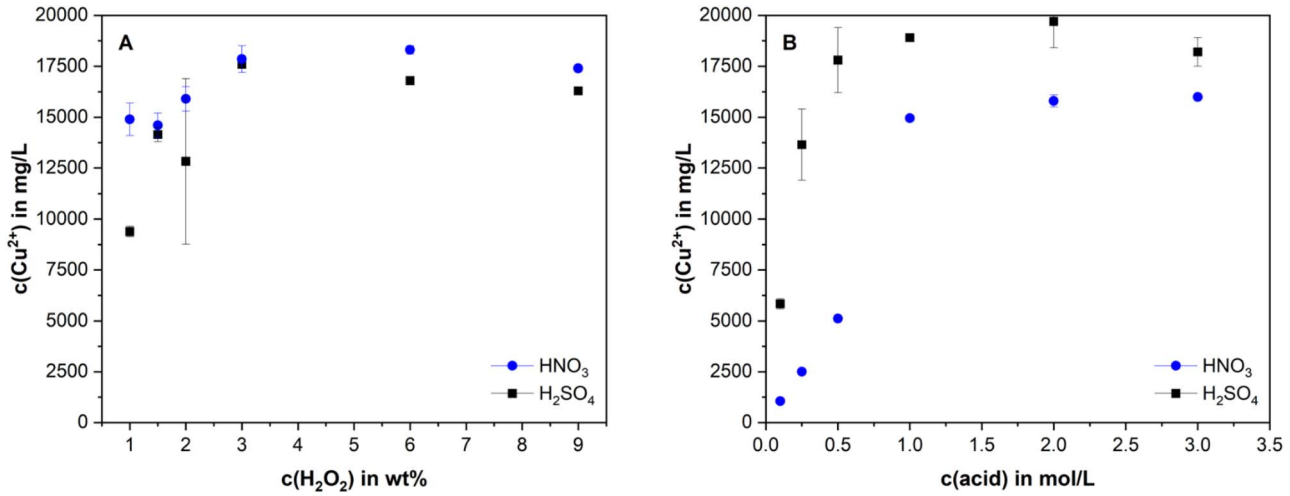

Fig. 4 Leaching of copper (concentration in mg L^{-1}) from PCB material in dependence on H_2O_2 concentration. (A) $c(H_2O_2) = 0$–9 wt%, $c(H_2SO_4) = c(HNO_3) = 3$ M, S/L = 1 : 10, $t = 4$ h, r.t. (B) Leaching of copper (concentration in mg L^{-1}) from PCB material in dependence on acid concentration. $c(H_2SO_4) = 0.1$–3 M, $c(H_2O_2) = 3$ wt%; $c(HNO_3) = 0.1$–3 M, S/L = 1 : 10, $t = 4$ h, r.t.

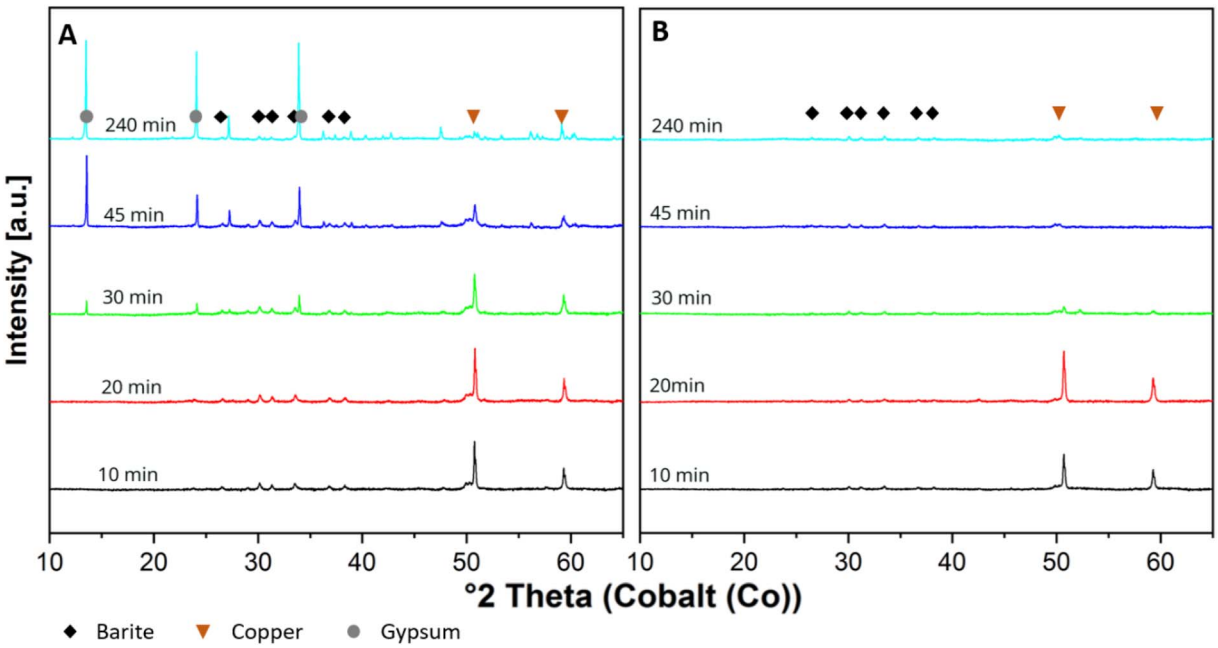

Fig. 5 XRD diffractograms of leaching residues ((A) H_2SO_4 and (B) HNO_3), illustrating the decreasing amount of copper in the residue material (copper-peaks at 50.8° and 59.3° 2theta, Co-radiation, additional main peaks of gypsum and barite are marked) depending on the reaction time. $c(H_2SO_4) = 3$ M, $c(H_2O_2) = 3$ wt%; $c(HNO_3) = 3$ M, S/L = 1 : 10, $t = 10$–240 min, r.t.

Similar approaches have been tested in the literature for the leaching of primary and secondary feeds, and H_2O_2 provides an excellent choice for the oxidative environment.[42] It has also been used along with additional parameters, such as ultrasound.[43] Also, the use of organic acids in the presence of hydrogen peroxide has been tested for the leaching of copper from PCBs.[44] Acid leaching followed by electrowinning has also been tested at low temperature and for the production of Cu nanoparticles.[45]

A series of leaching residues was subsequently characterized by XRD, the results of which are shown in Fig. 5. For the leaching system with H_2SO_4, a clear decrease in both peaks for copper was detected. From a reaction time of 30 min, however, peaks of $CaSO_4 \times 2H_2O$ (gypsum) occurred, which can be attributed to the reaction of dissolved calcium cations with sulfate. In contrast, in the case of HNO_3, as expected, only a reduction in the copper peaks was observed. In agreement with the experimental data from Fig. 5, these copper peaks are hardly detectable even after reaction times of 30 min in the HNO_3 system.

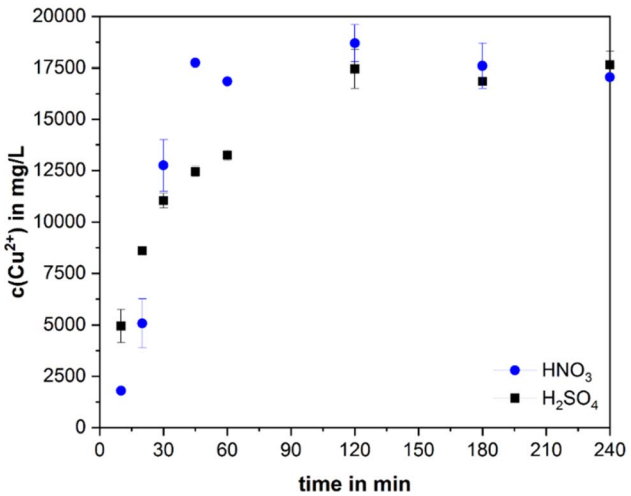

Fig. 6 Leaching of copper (concentration in mg L^{-1}) from PCB material in dependence on reaction time. $c(H_2SO_4) = 3$ M, $c(H_2O_2) = 3$ wt%; $c(HNO_3) = 3$ M, S/L = 1 : 10, $t = 10$ min-240 min, r.t.

In order to minimize the consumption of chemicals used and to achieve the highest possible concentration, the leaching processes were also investigated at different solid/liquid (s/l) phase ratios (Fig. 7A). A uniform increase in Cu^{2+} concentration was observed for HNO_3, so that Cu^{2+} extraction was independent of the phase ratio. In the case of the H_2SO_4/H_2O_2 leaching system, an increase in the copper concentration was also detected, although this was significantly lower than the theoretical maximum concentration. This can be attributed to a stoichiometrically lower amount of H_2SO_4 or the accelerated decomposition of H_2O_2.

To identify the cause of the reduced leaching yields of copper, additional studies were conducted to investigate the effects of acid concentration and H_2O_2. As shown in Fig. 7B, an increase in the H_2SO_4 concentration up to 4.5 M leads to a decrease in the leaching yields, contrary to expectations. It is assumed that increasing the acid concentration leads to a more rapid decomposition of H_2O_2 and a reduction in its reaction efficiency. Another possible explanation could be the accelerated formation of gypsum, which encapsulates individual particles after precipitation and hinders the reaction between the leaching medium and copper. It should be noted that the extraction of nickel (up to 816 mg L^{-1}) behaves analogously to

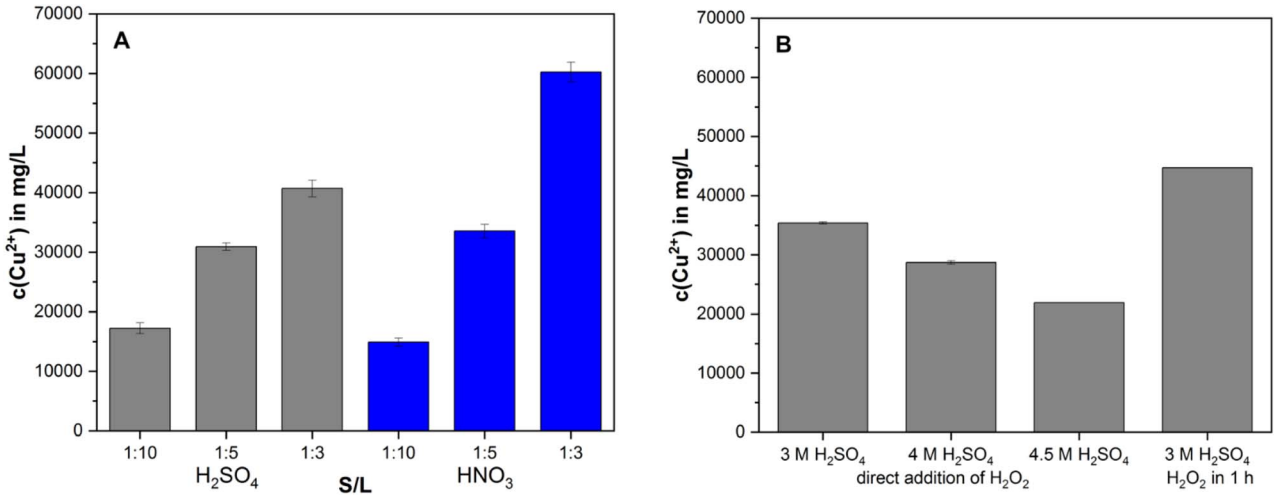

Fig. 7 (A) Concentration of Cu^{2+} (concentration in mg L^{-1}) from PCB material in leach solution in dependence of the solid-to-liquid ratio. $c(H_2SO_4) = 3$ M, $c(H_2O_2) = 3$ wt%; $c(HNO_3) = 3$ M, S/L = 1 : 10–1:3, $t = 240$ min, r.t. (B) Effect of H_2SO_4 concentration and direct or continuous H_2O_2 addition on leaching of copper (concentration in mg L^{-1}) from PCB material. $c(H_2SO_4) = 3$–4.5 M, $c(H_2O_2) = 3$ wt% (direct or in 1 h); S/L = 1 : 3, $t = 240$ min, r.t.

copper, whereas the Fe(III) concentration in the H_2SO_4/H_2O_2 leaching system is significantly higher (up to 143 mg L^{-1}) than in HNO_3 (70 mg L^{-1}). In further experiments, it was demonstrated that a continuous addition of H_2O_2 over a period of one hour leads to a significant increase in the leaching yields of copper in comparison to a direct addition of the oxidizing agent at the beginning of the experiment, which is attributed to the rapid decomposition due to exothermic reactions in the leaching process. In order to investigate the effect of particle size on the leaching performance, comparable studies have been carried out on material ranging in size from 630 μm to 1 mm (see Fig. S1 and Table S2). The preferred conditions in the two leaching systems are suitable for the complete dissolution of copper. However, due to the coarser particles in the feed material (obtained with industrial shredding range/conditions), the reaction time needed to be extended. On the other hand, the rapid decomposition of the oxidizer and formation of NOx can be minimized, and the filtration process is accelerated. This demonstrates the possible application of our optimized method in industrially relevant conditions.

3.3.1. Leaching under optimized conditions. The experimental conditions for two batch experiments were defined based on the results of the laboratory-scale studies. In the leaching system with H_2SO_4, its concentration was 3 M with 3 vol% H_2O_2 added over one hour, a total reaction time of four hours, and a phase ratio of 1 : 10. The continuous addition of H_2O_2 increases its effectiveness as an oxidizing agent, and the phase ratio and reaction time result in a higher than expected leaching yield for copper. In the case of HNO_3, an oxidizing agent was omitted, and a reaction time of 2.5 hours and a phase ratio of 1 : 3 were selected, since comparable leaching yields can be achieved under less intensive leaching conditions in terms of chemical ingredients and time requirements.

The leaching yields for copper and nickel are consistent with expectations from small-scale studies (Table 5). Based on the results of total digestion with HF, the extraction rate for the leaching system with sulfuric acid was at least 84.6% (copper) and 75.8% (nickel), and for the leaching system with HNO_3, at least 91.4% (copper) and 80.1% (nickel). Gold could only be detected for leaching with HNO_3, although in this case, the yield was only 1.2%. Notably, the higher concentration of Ca^{2+} in the leachate of HNO_3 is attributed to the limited solubility of gypsum (representing Ca-sulfate) in the abundance of H_2SO_4. Although a higher concentration of Cu^{2+} is obtained for the experiment with HNO_3, a technological challenge arises in the experiment. Only 22.7 mL (66%) of the originally used total volume could be separated from the leaching residue by centrifugation and decantation. This highlights the importance of an effective filtration process and limits the actual leaching yield for further metal recovery. In contrast, 90% of the pregnant leaching solution (PLS) could be obtained in the H_2SO_4/H_2O_2 leaching system. To increase the copper yield, washing and cementation steps were accordingly introduced into the process. It should be noted that significant amounts of NOx were released during the leaching with HNO_3. This represents a considerable technical and environmental challenge for further process development. The addition of a further reactant (*e.g.*, H_2O_2) could contribute to a reduction in the formation of hazardous NOx gases observed in the case of HNO_3.

3.4. Solvent extraction

To extract copper from the leaching solutions, a commercial extraction system consisting of LIX 84-I with kerosene diluent [5] was used as the organic phase. An optimized phase ratio A/O = 1 : 3 per contact was used for the batch process to minimize the number of extraction steps. This was supplemented by an extraction step of A/O = 1 : 1 for completeness. The results of the SX step are shown in Table 6. The O/A ratio optimization for the extraction step has been shown on the basis of the McCabe–

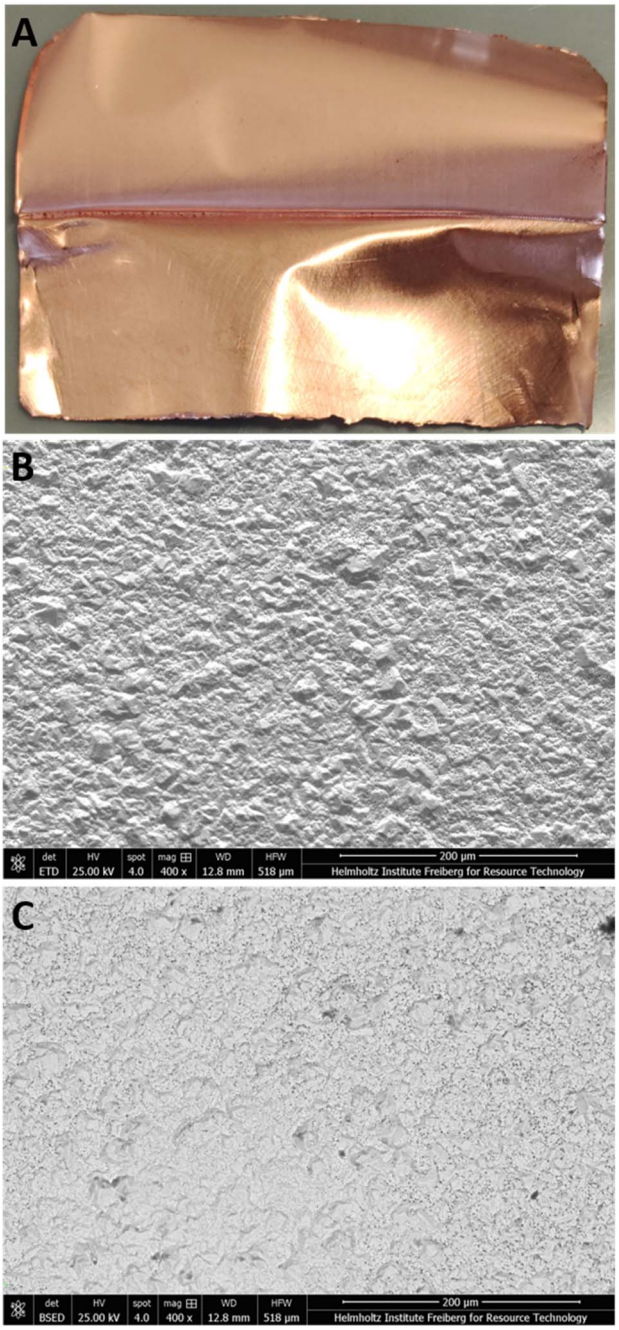

Fig. 8 (A) Deposit, (B) SEM and (C) backscattered image of copper deposit with sulfuric acid during EW. $C_{ini}(H_2SO_4) = 2$ M, CD = 30 mA cm^{-2}, $I = 0.6$ A, 1.98 V, $V = 400$ mL, $t = 240$ min, r.t.

Thiele diagram in SI Fig. S2 and S3. For the extraction system, LIX 84-I-kerosene/$CuSO_4$–H_2SO_4, >98% copper is transferred to the organic phase in a two-stage process. With the exception of Ni^{2+}, no co-extraction of further metal ions was detected. Due to the high initial concentration in the PLS containing HNO_3, an additional extraction step was necessary for the almost quantitative extraction of >96% of copper. In the subsequent stripping step, the two loaded organic phases were brought into contact with a model electrolyte, consisting of copper(II) sulfate

Table 5 Concentration of selected metal ions (in mg L^{-1}) in leach solutions after optimization of process parameters. $c(H_2SO_4) = 3$ M, $c(H_2O_2) = 3$ wt% (addition in 60 min), S/L = 1 : 10, $t = 240$ min., r.t.; $c(HNO_3) = 3$ M, S/L = 1 : 3, $t = 150$ min, r.t.; BDL: below detection limit

Leaching system	H_2SO_4	HNO_3
Metal ion	Concentration in mg L^{-1}	Concentration in mg L^{-1}
Cu^{2+}	17 400	62 700
Fe^{3+}	32.4	72.5
Ni^{2+}	229.5	808
Au^{3+}	BDL	0.002
Al^{3+}	2140	2120
Ca^{2+}	228	4080
Ba^{2+}	<2	<2
Si^{4+}	28.8	338

Table 6 Results of SX experiments for generated leachates. Extraction from H_2SO_4 leachate: 20 vol% LIX 84-I in kerosene, A/O = 1 : 3 (1×) + A/O = 1 : 1 (1×), pH_{eq} 1.47–1.79, $t = 15$ min., r.t.; extraction from HNO_3 leachate: 20 vol% LIX 84-I in kerosene, A/O = 1 : 3 (2×)+ A/O = 1 : 1 (1×), pH_{eq} 0.85–1.90, $t = 15$ min., r.t. pH adjustment with 10 M NaOH. Stripping: Cu^{2+} loaded 20 vol% LIX 84-I in kerosene, A/O = 0.8–1.2, 34.5 g L^{-1} Cu^{2+} in 2 M H_2SO_4, $t = 15$ min. BDL: below detection limit

Leaching system	H_2SO_4		HNO_3	
Metal ion	Extraction in %	Stripping in %	Extraction in %	Stripping in %
Cu^{2+}	98.23	97.15	96.11	98.79
Fe^{3+}	<0.1	BDL	35.13	>99
Ni^{2+}	39.78	>99	24.5	77.65
Au^{3+}	BDL	BDL	44%	BDL
Al^{3+}, Ca^{2+}, Ba^{2+}, Si^{4+}	<0.1	BDL	<0.1	BDL

in 2 mol L^{-1} H_2SO_4, to re-extract 97% and 98% copper, respectively. This was performed in order to maintain sufficient feed volume for the subsequent process step. The organic phase was then conditioned with 2 M H_2SO_4 to remove and quantify any remaining copper.

The ligand regeneration was monitored by FT-IR (Fig. 9). The absorption spectrum of the extraction system with the hydroxyoxime is characterized by a wide absorption band at 3400 cm^{-1} of the phenolic hydroxy function, the C=N stretching vibration at 1494 cm^{-1}, the C=N–OH deformation vibration at 1377 cm^{-1} of the hydroxyoxime group, and the O–H deformation vibration and C–O stretching vibration of the phenolic function (1200–1300 cm^{-1}). As a result of the chelate formation during the extraction of copper, the phenolic OH groups are no longer detected in the charged organic phase. During stripping, this group is protonated again, so the absorption bands reappear in the depleted organic phases.

3.5. Electrowinning

For the final production of metallic copper, the enriched electrolyte solutions were electrochemically treated for 4 hours in

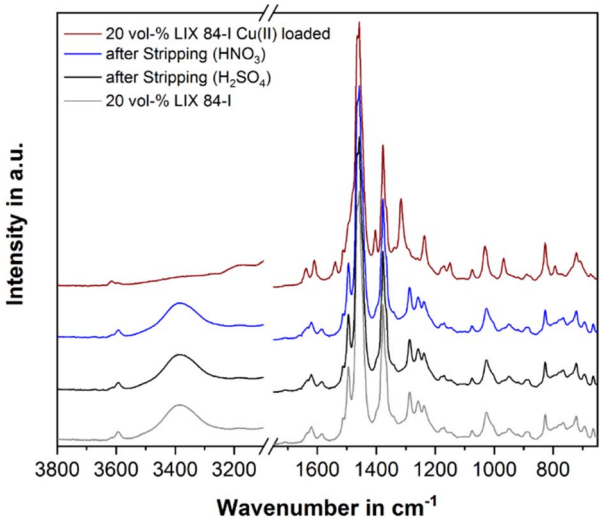

Fig. 9 FT-IR absorption spectra of 20 vol% LIX 84-I in kerosene, the Cu^{2+} loaded organic phase and the depleted organic phases after stripping.

a 400 mL electrolysis cell consisting of a stainless steel cathode and a lead anode. The decrease in the copper concentration and the development of the metal loading on the electrode of up to 25.1% and 20.7%, respectively, are shown in Fig. 10. Approximately 2.8 g of copper was generated in each case, which corresponds to a current efficiency of 99.85% (H_2SO_4 leaching system) and 98.66% (HNO_3 leaching system). This results in a slightly higher specific energy consumption of 1.69 kWh kg Cu for the HNO_3 leaching system compared to the H_2SO_4 leaching system (1.67 kWh kg Cu). With regard to the purity of the deposited copper, slight differences were detected (H_2SO_4: 99.84% copper, 0.06% iron, 0.04% nickel; HNO_3: 99.64% copper, 0.16% iron, 0.04% nickel) using EDX/EDS.

As a result of the SX process, small amounts of dissolved organic carbon were transferred to the electrolyte. During the

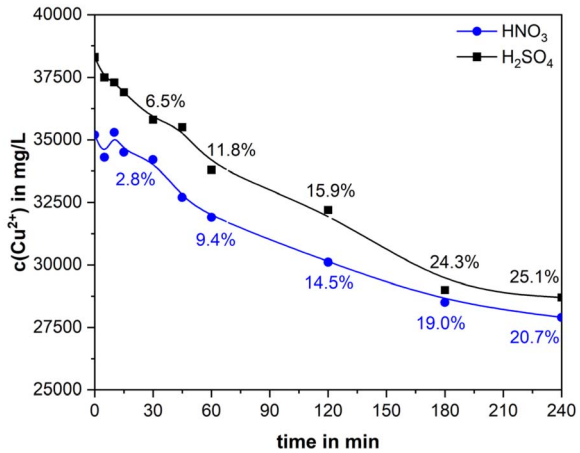

Fig. 10 Development of Cu^{2+} concentration (in mg L^{-1}) and metal loading (in %) for processed solutions from leaching with sulfuric acid and nitric acid during EW. $C_{ini}(H_2SO_4) = 2$ M, CD = 30 mA cm^{-2}, $I = 0.6$ A, 1.98 V, $V = 400$ mL, $t = 240$ min, r.t.

electrolysis process, some of the organic impurities were degraded. In the electrolyte from the H_2SO_4 leach, the TOC decreased from 84.0 ppm to 64.4 ppm, and in the case of the HNO_3 leach, from 74.0 ppm to 38.7 ppm. By introducing a prior purification step using activated carbon, the contamination of the electrolyte could be minimized. During the electrolysis process, H_2SO_4 was formed, which can be used in the stripping process to re-extract copper(II). The H_2SO_4 concentration increased from 1.88 M (H_2SO_4) and 1.85 M (HNO_3) to 1.99 M in each depleted electrolyte.

Fig. 8 shows the SEM and backscattered image of the Cu deposits. It is evident that the Cu plate is of high quality and smooth, suitable for further metal forming and end product utilization, *e.g.*, electric cable/PCB components manufacturing. Dendroid formation was not observed (Fig. S2 in SI). This helped us to establish the end-to-end approach for the Cu recovery.

The current densities were based on the overall electrolyte concentration for Cu ions as well as for the acid content. Also, the model electrolyte in the strip has been used to maintain this Cu concentration. The % removal of Cu indeed corresponds to the Cu arriving from PCB leachates and extractive steps. This has been ensured based on the 4 h of the electrowinning process time.

3.6. Washing and cementation

The leaching residues were subjected to a six-stage washing process to remove any remaining leached metal ions. Fig. 11 shows the development of the metal concentrations with the number of washing steps. The overall feed concentration was lower in comparison to the leach solution as the metal was diluted with washing water. The high concentrations of copper in the first three washing steps are still in the order of the concentration differences in the metal deposition process of electrolysis. Particularly in the case of HNO_3 leaching, the first wash step provides a possibility to significantly increase the copper recovery yield. All other metal ions were leached out to an extent similar to copper. The stable concentration of calcium in all wash solutions, based on the H_2SO_4 leaching, underscores its consistent solubility. This is due to a constant saturation of the solution with sparingly soluble gypsum ($CaSO_4 \times 2H_2O$).

In line with the expectations from the previous studies, metallic copper was no longer detected in the XRD diffractograms and was completely leached (Fig. 13). Barite and precipitated gypsum were observed in the washed leach residue after H_2SO_4 treatment. These results are confirmed by handheld XRF measurements (Table 7), which show that copper is no longer detectable and that both residues differ in particular with regard to the sulfur content, which is contained in the material in the form of gypsum.

In order to increase the copper yield, the solutions from the first three washing steps were subjected to a cementation process using iron powder as the reducing agent, and a Fe/Cu^{2+} ratio of 1.5 : 1 was selected in each case. The separated solid cements were analyzed by handheld XRF. The highest copper content was evaluated using the Cu/Fe ratio. It was observed that the Cu/Fe ratios generally decrease after each washing step.

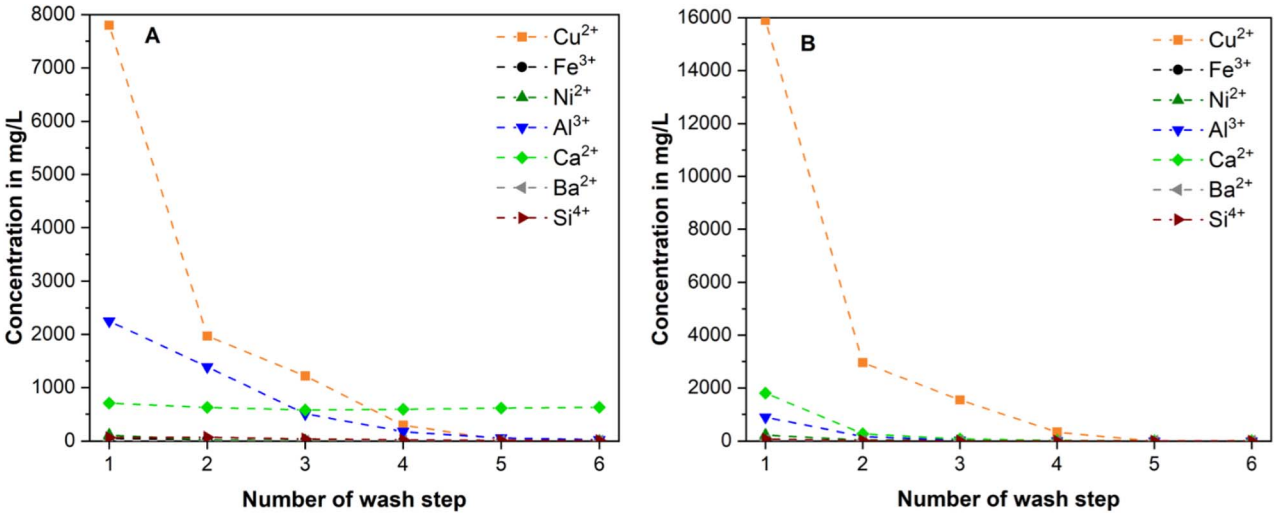

Fig. 11 Removal of remaining metal ions from leaching residues ((A) based on sulfuric acid leaching, (B) based on nitric acid leaching) of PCB material. Number of wash steps with water: 6, S/L = 1:3–1:2, t = 15 min per step, r.t.

For example, for H_2SO_4, the ratio decreases from 3.20 to 1.69 to 0.35. For HNO_3, the ratio decreases from 2.56 to 1.22 to 2.36. In addition, only small amounts (6–12%) of nickel were removed from the wash solution using the cementation process. The results presented in Fig. 12, based on ICP-OES of solutions, show that copper could be almost completely removed from the H_2SO_4 leaching system, especially for washing solutions. Although a larger amount of copper was recovered for the HNO_3 leaching system, the cementation process was less effective in terms of yield.

From the proposed flow-sheet (Fig. 1), gases like organic kerosene fumes and mineral acid fumes can be released. However, these are similar to industrial emissions, which are thoroughly assessed with LCA (Section 3.7). The safeguards, like a good exhaust gas system with gas treatments, are recommended. Also, liquid effluents as leachates and extraction raffinate, could be either reused, neutralized or treated using nanofiltration technology to mitigate the high liquid discharge.

3.7. Life cycle assessment

An LCA was conducted to compare the environmental sustainability of our hydrometallurgical copper recycling routes with the recycling routes of previous sustainability reports. In LCA, emissions are categorized into direct and indirect emissions. Here, only indirect emissions stemming from the production of consumed electricity and chemicals were considered to be relevant. The present study of hydrometallurgical leaching routes for copper recovery from PCBs has been conducted at laboratory scale only, with the goal of illustrating technical feasibility. Comminution of PCBs was only required to ascertain that all leaching experiments were done with aliquots of identical compositions. While the electricity requirement for comminution on such a small scale is highly inefficient, we've

Table 7 Elemental composition of the washed leaching residues. Data derived from handheld XRF

Leaching system	H_2SO_4	HNO_3
Element	wt%	wt%
Cu	<0.1	0.1
SiO_2	24.4	22.3
CaO	11.2	11.1
BaO	1.1	1.2
Al_2O_3	4.7	5
Ni	<0.1	<0.1
Au	<0.1	< 0.1
SO_3	11	0.1
Sum	52.5	39.8

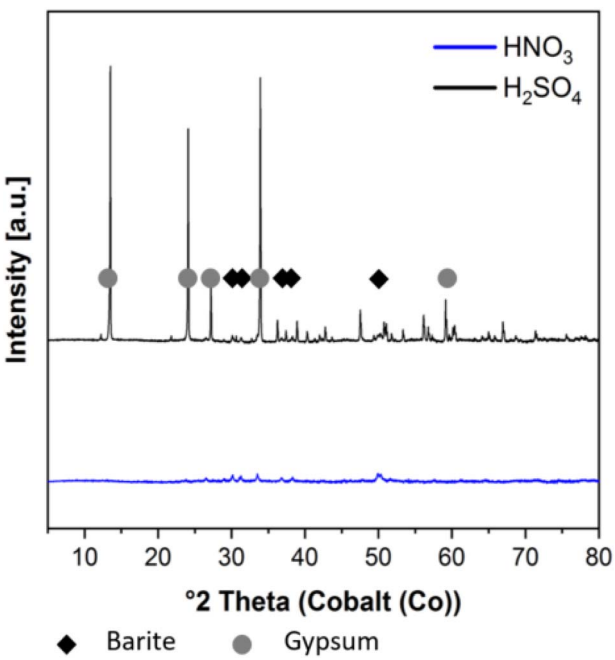

Fig. 12 XRD results of washing experiment series after leaching, illustrating the removal of copper in the residue material (Co-radiation, main peaks of gypsum and barite are marked).

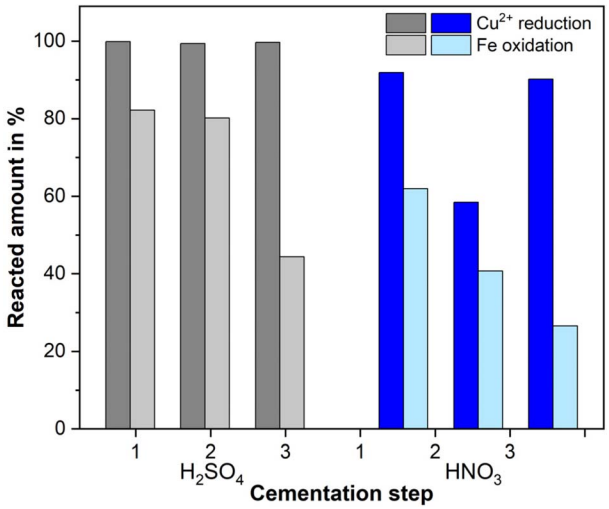

Fig. 13 Cementation of copper with iron powder from selected filtrates (based on wash steps 1, 2 and 3). $Fe/Cu^{2+} = 1.5:1$, 60 min, r.t.

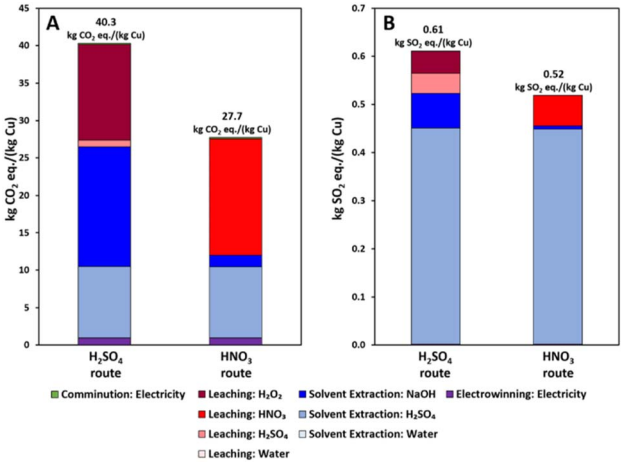

Fig. 14 Contribution of process units to [A] GWP100 and [B] TAP100 for copper recovery. In the current study, only indirect emissions were considered to be relevant. The emissions related to electricity consumption for comminution and water consumption for leaching and SX cumulatively contributed to <1% of GWP100 and TAP100 for both routes.

based our LCA study on the electricity requirement for industrial-scale shredding. Electricity consumption of shredders in the metal processing industry typically lies in the range 25–71 kWh per ton.[46] Here, we base our assumed consumption on a previous LCA study on WPCB recycling, which reported a combined electricity requirement of 43.9 kWh per ton for comminution using two crushers and a sieve.[47] During our experiments to assess the SX efficiency, the organic phase consisting of LIX 84-I with kerosene diluent was only used once. In an industrial setup, the organic phase would typically be recycled numerous times, thereby significantly decreasing the demand. As a result, the organic phase was not considered in our LCA.

3.7.1. Life cycle assessment without allocation factors. A detailed inventory for the production of copper cathodes was obtained from the experimental work performed within the scope of this study. Table S3 in SI shows LCIA mid-point assessment results, which indicate varying environmental impacts associated with the production of copper for both of the adopted hydrometallurgical routes (*i.e.*, H_2SO_4 and HNO_3) across different categories. The H_2SO_4 route consumes a significantly higher amount of reagents (*e.g.*, H_2SO_4, H_2O_2, and NaOH) and therefore demonstrates higher values for each of the 18 categories evaluated through the ReCiPe Midpoint (H) impact assessment method, as compared with the HNO_3 (Table S3).

The GWP100 serves as a crucial indicator for assessing the contribution of different processes to the emission of greenhouse gases, thus guiding the prioritization of mitigation efforts and the implementation of environmentally responsible practices within industries, such as metal or alloy production.[15] The contribution of each process unit/stage of the two copper production routes to GWP100 is shown in Fig. 14A. The overall emissions from the H_2SO_4 and HNO_3 routes are 40.30 and 27.73 kg CO_2 eq. per (kg Cu), respectively. The major process units causing emissions are leaching and SX, as both are characterized by high levels of reagent consumption. For instance, the H_2SO_4 route consumes a total of 12.69 kg NaOH, 65.50 kg H_2SO_4, and 8.76 kg H_2O_2 to produce 1 kg of copper.

In comparison, the HNO_3 route consumes 1.23 kg NaOH, 59.64 kg H_2SO_4, and 7.36 kg HNO_3 per functional unit. For the case of H_2SO_4, NaOH used in SX contributed 40% of overall emissions. Furthermore, H_2O_2 used in leaching contributed to 32% of overall emissions. Electricity used in the EW accounts for only around 2.3% and 3.4% of the emissions of H_2SO_4 and HNO_3 routes, respectively.

The TAP100 is a critical environmental impact category in LCA that measures the potential of emissions to cause acidification of terrestrial ecosystems over a 100-year time horizon. Acidification occurs when acidifying substances, primarily SO_x, NO_x, and NH_3, are released into the atmosphere. The contribution of each unit process for both the routes involved in the production of copper to TAP100 is shown in Fig. 14B. The overall emissions of the H_2SO_4 and HNO_3 routes are 0.61 and 0.52 kg SO_2 eq. per (kg Cu), respectively. The TAP100 for the H_2SO_4 route is 18% higher than for the HNO_3 route, which is again related to the high consumption of chemicals. The major unit contributing to the TAP100 is SX, contributing 85% and 87% for the H_2SO_4 and HNO_3 routes, respectively.

3.7.2. Life cycle assessment with economic allocation factors. The present study also explores economic allocation in LCA, which distributes the environmental impacts of processes among multiple products based on their market values. In recent years, this method has gained widespread acceptance among researchers due to its practicality and relevance.[15,48] In addition to the LCA discussed above, environmental impacts were allocated over the metals for the shared processing units, *i.e.*, shredding and leaching. Allocation factors were based on the product of the metals' contents (see Table 3), recoveries, and economic values. The latter were obtained by averaging the

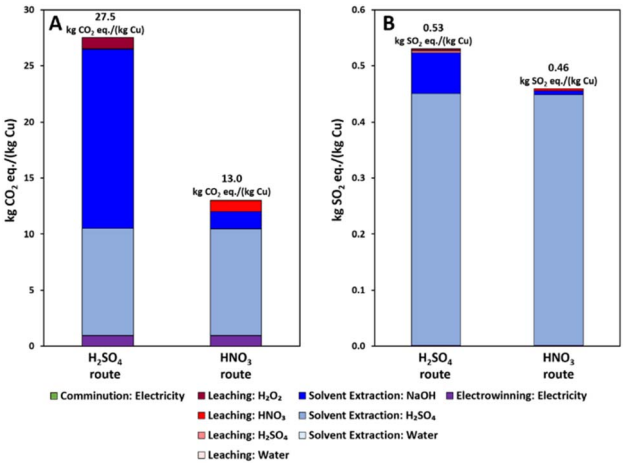

Fig. 15 Contribution of process units to (A) GWP100 and (B) TAP100 for copper recovery using the economic allocation method. In the current study, only indirect emissions were considered to be relevant. The emissions related to electricity consumption for comminution and water consumption for leaching and SX cumulatively contributed to <1% of GWP100 and TAP100 for both routes.

metals' market prices of the last five years: 7920 USD per ton of copper and 56 750 890 USD per ton_{gold}.[49] As the gold price is significantly higher than the copper price, approximately 92% share of the overall environmental burden of shredding and leaching is allocated to gold. In comparison, about 8% is allocated to copper. Hence, the GWP100 and TAP100 of the shared processing units (*i.e.*, shredding and leaching), considering economic allocation, represent lower values per functional unit, as shown in Fig. 15.

This increases the relative impact of other units, with the GWP100 for the H_2SO_4 route found to be 110% higher than for the HNO_3 route, due to more pronounced differences in SX. It is worth noting that a complete gold recovery was assumed for the calculation of the allocation factors. Although additional gold refining stages would be allocated to the environmental impacts related to gold and wouldn't impact the emission per functional unit, a partial gold recovery would decrease the allocation to gold and increase the allocation to copper. Therefore, while the scenarios under 3.7.1 overestimate the impacts of copper cathode production, the environmental impacts may be underestimated with the currently conducted economic allocation. Finally, other metals, such as nickel (27 900 USD per ton_{nickel},[49] 0.2 wt% (Table 3)), were also included alongside gold and copper, but yielded allocation factors of less than 0.5%.

A more common allocation practice involves making all system products available to the market and distributing the total burden based on their economic value. However, in this study, metals other than copper (*e.g.*, gold and nickel) remain in the leachates and are not readily available to the market. Accordingly, overall process allocation was avoided, and the burden of shared unit processes was allocated following the approach of Ardente and Celura (2012).[50]

3.7.3. Discussion and comparison to the literature. The results of the LCA with and without economic allocation suggest that the H_2SO_4 route is generally more impactful in terms of GWP100 and TAP100 compared to the HNO_3 route.

This can be attributed mainly to the ninefold higher use of NaOH related to aqueous phase conditions control and neutralization of dibasic H_2SO_4 acid. On the other hand, direct NO_X emissions from effluents (not considered here) can be avoided with the H_2SO_4 route compared to the HNO_3 route. Furthermore, it is possible to replace NaOH (31.5 kg CO_2 eq. per mol)[51] with environmentally benign Na_2CO_3 (4.3 kg CO_2 eq. per mol)[51,52] based neutralization in feasibility studies to reduce costs and impact, and retain the same process performance. Similarly, emissions due to the use of H_2O_2 (42.9 kg CO_2 eq. per mol)[51] in the H_2SO_4 route can be effectively reduced by increasing the molarity of H_2SO_4 (1.6 kg CO_2 eq. per mol).[51]

Most literature sources report values of approximately 1–5 kg CO_2 eq. per (kg Cu), as can be seen in Table 8. These differences are attributable to variations in starting material, *i.e.*, high-quality copper ore concentrate or copper scrap, research scope, beneficiation,[14] novel technology introduction[23] *vs.* industrial evaluation, geographic region of interest/operations, *e.g.*, Asian[15–17] *versus* European[14,20,53] copper production, system boundaries and LCA approaches, *e.g.*, gate-to-gate or cradle-to-gate, LCA software and database[20] or allocation techniques.[19]

It is evident from Table 8 that the hydrometallurgical routes explored in this study show roughly one order higher CO_2 impact compared to the pyrometallurgical route realized currently in industry and reported in literature. However, the capital expenditure required for hydrometallurgical plants is generally lower than pyrometallurgical plants.[54] In addition, hydrometallurgical plants are more easily scaled. Accordingly, a decentralized hydrometallurgical plant with low to medium throughput may still be a good option for copper recycling from PCBs, as it could reduce the CO_2 footprint and logistical complexity of WEEE processing. Moreover, the following aspects will help us to do a fair comparison: *e.g.*, for primary production from copper concentrate, the environmental impact of beneficiation (*ca.* 0.69 kg CO_2 eq. per (kg Cu)[14]) is not always accounted for. The reference point for calculations in gate-to-gate approaches is the point of entry to the metallurgical plant where copper production takes place. At this point, a primary raw material to be beneficiated will be a fine particulate material containing >20 wt% copper. In the case of PCBs as a recycling feed stream, copper content may be lower, but no physical beneficiation treatment will be applied to the PCBs prior to copper recovery. Therefore, recycling and hydrometallurgy processes may be more environmental friendly under these considerations.

Another important aspect is the fate of halogens. Halogenated compounds, such as chlorine and bromine, are invariably present in PCBs. These will ultimately end up in a liquid or solid residue stream during the hydrometallurgical copper recovery process. This residue may then be further processed for chemical and energy recovery. On the contrary, halogenated compounds report to the flue gas during the pyrometallurgical process. These compounds are toxic and highly corrosive. Consequently, additional measures are needed to treat such flue gas.

Table 8 Overview of LCA literature for copper production

Resource	Process	LCA approach	GWP100 in kg CO_2 eq. per (kg Cu)	References
Primary	Beneficiation of copper ore to copper concentrate	Cradle-to gate	0.69	(Song *et al.*, 2017)[14]
Primary	Pyrometallurgical	Gate-to-gate	7.65	(Kulczycka *et al.*, 2015)[18]
Primary	Pyrometallurgical	Cradle-to gate	1.91	(Hong *et al.*, 2018)[17]
Primary	Pyrometallurgical	Cradle-to gate	2.80	(Nuss & Eckelman, 2014)[19]
Primary	Pyrometallurgical	Cradle-to gate	3.51–4.75[a]	(Sanjuan-Delmás *et al.*, 2022)[20]
Primary	Pyrometallurgical	Cradle-to gate	5.88	(Dong *et al.*, 2020)[16]
Primary	Hydrometallurgy	Cradle-to gate	7.37	(Dong *et al.*, 2020)[16]
Secondary	Pyrometallurgical	Cradle-to gate	1.59	(Dong *et al.*, 2020)[16]
Primary	Pyrometallurgical	Cradle-to gate	3.42	(Chen *et al.*, 2019)[15]
Secondary	Pyrometallurgical	Cradle-to gate	0.32	(Chen *et al.*, 2019)[15]
Secondary	Pyrometallurgical	Cradle-to gate	0.69	(Hong *et al.*, 2018)[17]
Secondary	Pyrometallurgical	Gate-to-gate	1.46	(Torrubia *et al.*, 2024)[21]
Secondary	Pyrometallurgical	Cradle-to gate	1.58	(Van der Voet *et al.*, 2019)[22]
Secondary	Hydrometallurgy	Gate-to-gate	240.6[b]	(Rao *et al.*, 2023)[23]
Secondary	Hydrometallurgy	Gate-to-gate	173.6[c]	(Rao *et al.*, 2023)[23]
Secondary	Hydrometallurgy	Gate-to-gate	8.6[d]	(Rubin *et al.*, 2014)[24]
Primary and secondary	Pyrometallurgical	Cradle-to gate	1.46	(Aurubis, 2023)[53]
Secondary	Hydrometallurgy	Gate-to-gate	13.0–40.3	Current study

[a] 3.51 was obtained with GaBi software and databases, and 4.75 with the SimaPro software and Ecoinvent database. [b] In the work by Rao *et al.*, the final copper had an inferior quality (93.57% copper purity, 6.26% oxygen, dendritic structure) to the product in our study. Furthermore, for comparability to our LCA with negligible contribution of shredding, we did not consider emissions reported by Rao *et al.* for delamination. [c] Not considering delamination and with an economic allocation of 8% (similar to the current study) to copper for emissions related to leaching. [d] Value mentioned here for H_2SO_4 route.

When comparing the GWP of the process presented in this work to other hydrometallurgical processes for copper recycling from PCBs, we report comparable performances relative to Rubin *et al.* (2024)[24] and significantly better than Rao *et al.* (2023).[23] Finally, it is important to note that scaling up the presented technical process will increase efficiency and hence reduce the CO_2 footprint per kg of product. Further impact reduction can be achieved *via* process optimization in terms of electricity consumption, chemical usage, and considering alternative or lower-impact chemicals. Additionally, transitioning to renewable energy sources for electricity could provide significant reductions in the environmental impact.

4. Conclusions

The successful demonstration of end-to-end copper recovery from virgin PCBs involved near quantitative leaching using dual leaching routes of H_2SO_4 and HNO_3. The thorough understanding of PCB feeds and detailed characterization of residues contributed to the design and implementation of oxidative conditions, which resulted in >98% copper enriched in the stripping phase. Subsequently, it was converted to solid metallic copper with a purity of 99.64–99.84% by EW with an impressive current efficiency of 98.66–99.85%. The comparison to industrially relevant shredding conditions showed higher Cu recovery after leaching time-based optimizations. Detailed LCA studies based on the developed process indicate emissions in the range 13.0–40.3 kg CO_2 eq. per (kg Cu), comparable to those of conventional pyrometallurgical operations. These values are reasonable in comparison to the impact of copper recycling processes on an industrial scale. This shows the need to find mechanisms and efficient scale–up parameters – in order to link industrial process data to lab-scale innovation. We have demonstrated such a correlation by choosing suitable end-to-end and scalable process steps, LCA boundary conditions for the reported hydrometallurgical process. The CO_2 eq impact can further vary and be optimized based on direct sustainability due to the reuse of process ingredients, composition of feed PCBs, allocation to metal values, and mechanical processing/shredding and transport complexity.

Author contributions

Conceptualization: NK, PB, AMP, ABP and JG; methodology: NK, PB, SK, DE, BG, RM MA, CS-G, UF, MS, AR, LO, FE and ABP; validation: NK, PB, AMP, RM, FE, AR and ABP; formal analysis: DE, BM, CS-Gm UF and MS; investigation: NK, PB, AMP, RM, LO and ABP; resources: AR, JG, NK, RM, ABP and JG; data curation: NK, AMP and PB; roles/writing – original draft: NK, PB, AMK, MS, ABP and RM; writing – review & editing: NK, PB, AMP, RM, MS, FE, ABP and JG; visualization: NK, PB, RM, BG, DE, CS-G, UF and ABP; supervision: ABP, AR and JG; project administration: NK and PB; funding acquisition: PB, AMP and JG.

Conflicts of interest

The authors declare that there are no conflicts of interest.

Data availability

The data supporting this article have been included as part of the supplementary information (SI). Supplementary information: supplementary data, and further clarification on LCA databases. See DOI: https://doi.org/10.1039/d5va00348b.

Acknowledgements

The authors would like to thank Roland Würkert for sample preparation, Lucas Pereira for supervision, Dominic Illing for CHNS analysis, Chaouki Boucena for support with acid titration, SEM preparation, and TOC, Stefanie Schubert for ICP-OES measurements, Sabrina Beutner for ICP-MS measurements, Rocco Naumann and Abrar Kabir for assistance with comminution.

References

1 C. P. Baldé, R. Kuehr, T. Yamamoto, R. McDonald, E. D'Angelo, S. Althaf, G. Bel, O. Deubzer, E. Fernandez-Cubillo, V. Forti, V. Gray, S. Herat, S. Honda, G. Iattoni, D. S. Khetriwal, V. Luda di Cortemiglia, Y. Lobuntsova, I. Nnorom, N. Pralat and M. Wagner, *The Global E-Waste Monitor 2024*, International Telecommunication Union (ITU) and United Nations Institute for Training and Research (UNITAR), 2024.

2 X. Zeng, L. Zheng, H. Xie, B. Lu, K. Xia, K. Chao, W. Li, J. Yang, S. Lin and J. Li, Current Status and Future Perspective of Waste Printed Circuit Boards Recycling, *Procedia Environ. Sci.*, 2012, **16**, 590–597.

3 L. Maria Paola, in *Integrated Waste Management*, ed. K. Sunil, IntechOpen, Rijeka, 2011, p. 15, DOI: 10.5772/17220.

4 M. Oguchi, S. Murakami, H. Sakanakura, A. Kida and T. Kameya, A preliminary categorization of end-of-life electrical and electronic equipment as secondary metal resources, *Waste Manage.*, 2011, **31**, 2150–2160.

5 H. Long Le, J. Jeong, J.-C. Lee, B. D. Pandey, J.-M. Yoo and T. H. Huyunh, Hydrometallurgical Process for Copper Recovery from Waste Printed Circuit Boards (PCBs), *Miner. Process. Extr. Metall. Rev.*, 2011, **32**, 90–104.

6 European Commission, *Study on the Critical Raw Materials for the EU 2023 – Final Report*, 2023.

7 H. M. Veit, A. M. Bernardes, J. Z. Ferreira, J. A. S. Tenório and C. D. F. Malfatti, Recovery of copper from printed circuit boards scraps by mechanical processing and electrometallurgy, *J. Hazard. Mater.*, 2006, **137**, 1704–1709.

8 Y. F. Guimarães, I. D. Santos and A. J. B. Dutra, Direct recovery of copper from printed circuit boards (PCBs) powder concentrate by a simultaneous electroleaching–electrodeposition process, *Hydrometallurgy*, 2014, **149**, 63–70.

9 R. Mathaiyan, M. S. Shabanur Matada, Y. Sivalingam and S. Kancharla, Copper Recovery from Mobile Phone Printed Circuit Board E-Waste and Transforming into CuO@C for Electrode Material in Extended Gate Field-Effect Transistors Facilitating Non-Enzymatic Ascorbic Acid Detection, *ACS Sustain. Chem. Eng.*, 2024, **12**, 10752–10764.

10 A. B. Patil, R. P. W. J. Struis and C. Ludwig, Opportunities in Critical Rare Earth Metal Recycling Value Chains for Economic Growth with Sustainable Technological Innovations, *Circ. Econ. Sustainability*, 2023, **3**, 1127–1140.

11 P. Boelens, L. Pereira, K. Tumakov, J. R. da Assuncao Godinho, C. G. da Silva Tochtrop, S. Gupta, B. M. Guy, R. Tolosana-Delgado, R. Möckel, T. Leißner, E. Löwer, D. Illing, A. D. Renno, L. Ott, F. Ellinger, M. Rudolph and J. Gutzmer, A workflow to assess the recoverability of secondary raw materials *via* physical separation, *Waste Manage.*, 2025, **193**, 561–570.

12 ISO, *14040; Environmental Management; Life Cycle Assessment; Principles and Framework*, International Organization for Standardization, Geneva, Switzerland, 2006.

13 R. Memary, D. Giurco, G. Mudd and L. Mason, Life cycle assessment: a time-series analysis of copper, *J. Cleaner Prod.*, 2012, **33**, 97–108.

14 X. Song, J. B. Pettersen, K. B. Pedersen and S. Røberg, Comparative life cycle assessment of tailings management and energy scenarios for a copper ore mine: A case study in Northern Norway, *J. Cleaner Prod.*, 2017, **164**, 892–904.

15 J. Chen, Z. Wang, Y. Wu, L. Li, B. Li, D. a. Pan and T. Zuo, Environmental benefits of secondary copper from primary copper based on life cycle assessment in China, *Resour., Conserv. Recycl.*, 2019, **146**, 35–44.

16 D. Dong, L. van Oers, A. Tukker and E. van der Voet, Assessing the future environmental impacts of copper production in China: Implications of the energy transition, *J. Cleaner Prod.*, 2020, **274**, 122825.

17 J. Hong, Y. Chen, J. Liu, X. Ma, C. Qi and L. Ye, Life cycle assessment of copper production: a case study in China, *Int. J. Life Cycle Assess.*, 2018, **23**, 1814–1824.

18 J. Kulczycka, L. Lelek, A. Lewandowska, H. Wirth and J. Bergesen, Environmental Impacts of Energy-Efficient Pyrometallurgical Copper Smelting Technologies: The Consequences of Technological Changes from 2010 to 2050, *J. Ind. Ecol.*, 2015, **20**(2), 304–316.

19 P. Nuss and M. Eckelman, Life Cycle Assessment of Metals: A Scientific Synthesis, *PLoS One*, 2014, **9**, e101298.

20 D. Sanjuan-Delmás, R. A. F. Alvarenga, M. Lindblom, T. C. Kampmann, L. van Oers, J. B. Guinée and J. Dewulf, Environmental assessment of copper production in Europe: an LCA case study from Sweden conducted using two conventional software-database setups, *Int. J. Life Cycle Assess.*, 2022, **27**, 255–266.

21 J. Torrubia, A. M. S. Parvez, M. Sajjad, F. A. V. García Paz and K. G. van den Boogaart, Recovery of copper from electronic waste: An energy transition approach to decarbonise the industry, *J. Cleaner Prod.*, 2024, **485**, 144349.

22 E. Van der Voet, L. Van Oers, M. Verboon and K. Kuipers, Environmental implications of future demand scenarios for metals: methodology and application to the case of seven major metals, *J. Ind. Ecol.*, 2019, **23**, 141–155.

23 M. D. Rao, R. B. Meshram, K. K. Singh, C. A. Morrison and J. B. Love, Life cycle analysis on sequential recovery of copper and gold from waste printed circuit boards, *Waste Manage.*, 2023, **171**, 621–627.
24 R. S. Rubin, M. A. S. D. Castro, D. Brandão, V. Schalch and A. R. Ometto, Utilization of Life Cycle Assessment methodology to compare two strategies for recovery of copper from printed circuit board scrap, *J. Cleaner Prod.*, 2014, **64**, 297–305.
25 A. M. Cromwick, G. A. Birrer and R. A. Gross, Effects of pH and aeration on gamma-poly(glutamic acid) formation by Bacillus licheniformis in controlled batch fermentor cultures, *Biotechnol. Bioeng.*, 1996, **50**, 222–227.
26 S. Papanikolaou, L. Muniglia, I. Chevalot, G. Aggelis and I. Marc, Yarrowia lipolytica as a potential producer of citric acid from raw glycerol, *J. Appl. Microbiol.*, 2002, **92**, 737–744.
27 M. Sajjad, K. Van den Boogaart, L. Steinmeier and A. Parvez, Environmental Impact Assessment of Copper-Alloy Production Using Process Simulation and Semantic Modeling, *Adv. Eng. Mater.*, 2025, **27**, 2401702.
28 X. Song, J. Yang, B. Lu, B. Li and G. Zeng, Identification and assessment of environmental burdens of Chinese copper production from a life cycle perspective, *Front. Environ. Sci. Eng.*, 2014, **8**, 580–588.
29 K. Stem and E. J. S. Weise, *National Bureau of Standards Bulletin, High Temperature Properties and Decomposition of Inorganic Salts, Part I*, 1966, p. 7.
30 S. T. Abhilash, A. Ghosh, P. Meshram and E. D. van Hullebusch, Microbial Processing of Waste Shredded PCBs for Copper Extraction Cum Separation—Comparing the Efficacy of Bacterial and Fungal Leaching Kinetics and Yields, *Metals*, 2021, **11**, 317.
31 A. Becci, A. Amato, V. Fonti, D. Karaj and F. Beolchini, An innovative biotechnology for metal recovery from printed circuit boards, *Resour., Conserv. Recycl.*, 2020, **153**, 104549.
32 A. Işıldar, J. van de Vossenberg, E. R. Rene, E. D. van Hullebusch and P. N. L. Lens, Two-step bioleaching of copper and gold from discarded printed circuit boards (PCB), *Waste Manage.*, 2016, **57**, 149–157.
33 F. Faraji, R. Golmohammadzadeh, F. Rashchi and N. Alimardani, Fungal bioleaching of WPCBs using Aspergillus niger: Observation, optimization and kinetics, *J. Environ. Manage.*, 2018, **217**, 775–787.
34 D. Kaliyaraj, M. Rajendran, V. Angamuthu, A. Renita, M. Kaari, T. Shanmugasundaram, V. Gopikrishnan, J. Joseph and M. Radhakrishnan, Bioleaching of heavy metals from printed circuit board (PCB) by Streptomyces albidoflavus TN10 isolated from insect nest, *Bioresour. bioprocess.*, 2019, **6**, 47.
35 M. E. Díaz-Martínez, R. Argumedo-Delira, G. Sánchez-Viveros, A. Alarcón and M. R. Mendoza-López, Microbial Bioleaching of Ag, Au and Cu from Printed Circuit Boards of Mobile Phones, *Curr. Microbiol.*, 2019, **76**, 536–544.
36 É. F. Rodrigues, B. Cesa Rovaris, A. Valerio, D. de Oliveira and D. Hotza, Bioleaching of Printed Circuit Board Waste to Obtain Metallic Nanoparticles, *Sustainability*, 2024, **16**, 9837.
37 V. Beiki, T. Naseri and S. M. Mousavi, An efficient approach for enhancement of gold and silver bioleaching from spent telecommunication printed circuit boards using cyanogenic bacteria: Prevention of biofilm formation, *Waste Manage.*, 2023, **171**, 590–598.
38 T. D. Chi, J.-C. Lee, B. D. Pandey, K. Yoo and J. Jeong, Bioleaching of gold and copper from waste mobile phone PCBs by using a cyanogenic bacterium, *Miner. Eng.*, 2011, **24**, 1219–1222.
39 G. Merli, A. Becci and A. Amato, Recovery of precious metals from printed circuit boards by cyanogenic bacteria: Optimization of cyanide production by statistical analysis, *J. Environ. Chem. Eng.*, 2022, **10**, 107495.
40 G. Natrajan and Y. P. Ting, Two-Step Bioleaching and Spent Medium Leaching of Gold from Electronic Scrap Material Using Chromobacterium violaceum, *Adv. Mater. Res.*, 2013, **825**, 270–273.
41 J. Pradhan and S. Kumar, *Metals Bioleaching from Electronic Waste by Chromobacterium Violaceum and Pseudomonads Sp, Waste Management & Research : the Journal of the International Solid Wastes and Public Cleansing Association*, ISWA, 2012, vol. 30.
42 M. J. Nicol, The role and use of hydrogen peroxide as an oxidant in the leaching of minerals. 1. acid solutions, *Hydrometallurgy*, 2020, **193**, 105328.
43 G. Sun, M. Jiang, S. Wang, Y. Zuo, G. Zhang, Z. Hu and L. Zhang, The ultrasound leaching kinetics of copper in the H_2SO_4 dissolution process, *Can. Metall. Q.*, 2024, **64**, 1–15.
44 J. He, M. Zhang, H. Chen, S. Guo, L. Zhu, J. Xu and K. Zhou, Enhancement of leaching copper by organic agents from waste printed circuit boards in a sulfuric acid solution, *Chemosphere*, 2022, **307**, 135924.
45 M. A. R. Khan and H. M. M. A. Rashed, Selective recovery of nanoscale copper particles from mobile phone waste printed circuit boards through acid leaching and low temperature electrowinning, *Sci. Rep.*, 2025, **15**, 23195.
46 Sicon, *Data Sheet EcoShred® Vertec*, available online: https://sicontechnology.com/wp-content/uploads/ecoshred-vertec-e.pdf, accessed on 7 October 2024, 2024.
47 P. Pokhrel, S.-L. Lin and C.-T. Tsai, Environmental and economic performance analysis of recycling waste printed circuit boards using life cycle assessment, *J. Environ. Manage.*, 2020, **276**, 111276.
48 A. Ekman Nilsson, M. Macias Aragonés, F. Arroyo Torralvo, V. Dunon, H. Angel, K. Komnitsas and K. Willquist, A Review of the Carbon Footprint of Cu and Zn Production from Primary and Secondary Sources, *Minerals*, 2017, **7**, 168.
49 TradingEconomics, *Trading Economics Price of Metals*, available online: https://tradingeconomics.com/commodities, accessed on 24 June 2024, 2024.
50 F. Ardente and M. Cellura, Economic allocation in life cycle assessment: the state of the art and discussion of examples, *J. Ind. Ecol.*, 2012, **16**, 387–398.
51 Ecoinvent, *Ecoinvent Life Cycle Inventory Database v3.8*, Swiss Centre for Life Cycle Inventories, available: http://www.ecoinvent.ch/. Accessed 25 September 2024, 2021.

52 CarbonCloud, *Technical Report - Climate Footprint of Sodium Carbonate (Na_2CO_3). E500*, available online: https://apps.carboncloud.com/climatehub/product-reports/id/44158023257, accessed on 7 October 2024, 2024.
53 Aurubis, Environmental Footprint Declaration, *Aurubis Copper Cathode Report*, available at: https://www.aurubis.com/, accessed 09 December 2025.
54 R. Woeste, E.-S. Drude, D. Vrucak, K. Klöckner, E. Rombach, P. Letmathe and B. Friedrich, A techno-economic assessment of two recycling processes for black mass from end-of-life lithium-ion batteries, *Appl. Energy*, 2024, **361**, 122921.